Critical dynamics of self-gravitating Langevin particles and bacterial populations

Clément Sire and Pierre-Henri Chavanis
Laboratoire de Physique Théorique-IRSAMC, CNRS, Université Paul Sabatier, 31062 Toulouse, France
(Received 23 April 2008; published 11 December 2008)

We study the critical dynamics of the generalized Smoluchowski-Poisson system (for self-gravitating Langevin particles) or generalized Keller-Segel model (for the chemotaxis of bacterial populations). These models [P. H. Chavanis and C. Sire, Phys. Rev. E **69**, 016116 (2004)] are based on generalized stochastic processes leading to the Tsallis statistics. The equilibrium states correspond to polytropic configurations with index n similar to polytropic stars in astrophysics. At the critical index $n_3=d/(d-2)$ (where $d\geqslant 2$ is the dimension of space), there exists a critical temperature Θ_c (for a given mass) or a critical mass M_c (for a given temperature). For $\Theta>\Theta_c$ or $M<M_c$ the system tends to an incomplete polytrope confined by the box (in a bounded domain) or evaporates (in an unbounded domain). For $\Theta<\Theta_c$ or $M>M_c$ the system collapses and forms, in a finite time, a Dirac peak containing a finite fraction M_c of the total mass surrounded by a halo. We study these regimes numerically and, when possible, analytically by looking for self-similar or pseudo-self-similar solutions. This study extends the critical dynamics of the ordinary Smoluchowski-Poisson system and Keller-Segel model in $d=2$ corresponding to isothermal configurations with $n_3\to+\infty$. We also stress the analogy between the limiting mass of white dwarf stars (Chandrasekhar's limit) and the critical mass of bacterial populations in the generalized Keller-Segel model of chemotaxis.

DOI: 10.1103/PhysRevE.78.061111 PACS number(s): 05.90.+m, 05.40.−a, 47.20.−k, 05.70.−a

I. INTRODUCTION

For a long time, statistical mechanics was restricted to systems interacting via short-range forces. For example, the case of self-gravitating systems is almost never considered in standard textbooks of statistical mechanics and these systems have been studied exclusively in the context of astrophysics. In the sixties, Antonov [1], Lynden-Bell [2], and Thirring [3] realized that self-gravitating systems have a very special thermodynamics marked by the nonequivalence of statistical ensembles (microcanonical, canonical, grand canonical,…). This is related to the nonadditivity of the energy and to the presence of negative specific heats in the microcanonical ensemble. Furthermore, these systems experience a rich diversity of phase transitions (microcanonical and canonical first-order phase transitions, zero-order phase transitions,…) associated with their natural tendency to undergo gravitational collapse [4,5]. Recently, several researchers have started to consider the dynamics and thermodynamics of systems with long-range interactions at a more general level (see the books [6,7] and references therein) and to discuss the numerous analogies (and differences) between these systems: self-gravitating systems, two-dimensional vortices, neutral and non-neutral plasmas, the Hamiltonian mean field (HMF) model, free electron lasers, Bose-Einstein condensates, atomic clusters, chemotaxis of bacterial populations, etc. These analogies have also suggested interesting experiments. For example, in the physics of ultracold gases, some authors [8] have proposed to generate an attractive $1/r$ interaction between atoms by using a clever configuration of laser beams. This leads to the fascinating possibility of reproducing, in the laboratory, the *isothermal collapse* (in the canonical ensemble) of a self-gravitating Fermi gas [9,10] leading to a "white dwarf star." These examples illustrate the importance of studying the statistical mechanics of systems with long-range interactions at a general level and to develop the analogies between different systems that may seem *a priori* of a very different nature.

In a series of papers [11–17], we have investigated the dynamics and thermodynamics of a system of self-gravitating random walkers. The basic idea is to couple the usual Brownian motion (as introduced by Einstein and Smoluchowski) to the gravitational interaction. In our general model [17], the microscopic dynamics of the particles is described by N coupled stochastic equations including a friction force and a stochastic force in addition to the gravitational interaction. The friction force and the stochastic force model the interaction of the system with a thermal bath of nongravitational origin. Then, the proper statistical description of this *dissipative* system is the canonical ensemble. In order to simplify the problem, we have considered a strong friction limit in which the motion of the particles is overdamped. We have also considered a mean field approximation which becomes exact in a proper thermodynamic limit $N\to+\infty$ in such a way that the volume $V\sim 1$ is of order unity and the coupling constant $G\sim 1/N$ goes to zero (alternatively, we can consider that the mass of the individual particles scales like $m\sim 1/N$ so that the total mass $M\sim Nm$ and the gravity constant G remain of order unity). These approximations lead to the Smoluchowski-Poisson (SP) system. The steady states correspond to isothermal distributions associated with the Boltzmann statistics. When coupled to the Poisson equation, we obtain density profiles similar to *isothermal stars* in astrophysics [18,19]. In the course of our study, we realized that the SP system is isomorphic to the standard Keller-Segel (KS) model [20,21] introduced in mathematical biology to describe the chemotaxis of bacterial populations [22]. The SP system and the KS model have now been extensively studied by physicists [11–17,23] and applied mathematicians [24–47] with different methods and motivations.

We have also studied a generalized Smoluchowski-Poisson (GSP) system [see Eqs. (13) and (14) of this paper]

including an arbitrary barotropic equation of state $P(\rho)$. This model has been introduced by Chavanis in [48]. The GSP system can be viewed as a generalized mean field Fokker-Planck equation (for a review of nonlinear Fokker-Planck equations, see [49,50]). It can be obtained from generalized stochastic processes and it is associated with a notion of effective generalized thermodynamics (EGT). These equations can also provide a generalized Keller-Segel (GKS) model of chemotaxis with a density dependent diffusion coefficient [50]. For an isothermal equation of state $P=\rho k_B T/m$, we recover the standard SP system and KS model (with appropriate notations). Apart from the isothermal equation of state, the GSP system and GKS model have been studied for (i) a polytropic equation of state $P=K\rho^{\gamma}$ [51], (ii) a logotropic equation of state $P=A\ln\rho$ [52], (iii) a Fermi-Dirac equation of state $P=P_{F.D.}(\rho)$ [53,54], and (iv) an equation of state $P=-T\rho_{max}\ln(1-\rho/\rho_{max})$ taking into account excluded volume effects [55]. These are standard equations of state introduced in astrophysics and statistical mechanics so that it is natural to consider these equations of state in connection to the GSP system and GKS model.

Specializing on the polytropic equation of state $P=K\rho^{\gamma}$ with $\gamma=1+1/n$ [51], the steady states of the GSP system correspond to polytropic distributions associated with the Tsallis statistics [56]. When coupled to the Poisson equation, we obtain density profiles similar to *polytropic stars* in astrophysics [18,19]. For $d\geqslant 2$, there exists a critical index $\gamma_{4/3}=2(d-1)/d$, i.e., $n_3=d/(d-2)$ [51]. For $0<n<n_3$, the GSP system relaxes towards a stable steady state with a compact support, similar to a classical white dwarf star (classical white dwarf stars are equivalent to polytropes with index $n=3/2$ in $d=3$ [57]). For $n>n_3$, there is no stable equilibrium in an unbounded domain so that the system can either collapse or evaporate (see Fig. 13 for an illustration). These different regimes have been studied in [51]. For $n=n_3$, the dynamics is critical. At this index, there exists a critical mass $M_c(d)$ (for a given polytropic constant K) [51] which is connected to the Chandrasekhar mass of relativistic white dwarf stars (ultrarelativistic white dwarf stars are equivalent to polytropes with index $n=3$ in $d=3$ [58]). The object of the present paper is to study numerically and, when possible, analytically this critical dynamics. For $M<M_c$, we find that the system evaporates and we construct a self-similar solution. For $M>M_c$, we find that the system collapses. In a finite time t_{coll}, it forms a Dirac peak with mass M_c surrounded by a halo that has a pseudo-self-similar evolution. For $d=2$, the critical index $n_3\to+\infty$ so that we recover the case of isothermal spheres whose dynamics is known to be critical in $d=2$ [12].

When we apply this model in the context of chemotaxis [59], we find the existence of a critical mass $M_c(d)$ at the critical index $n_3=d/(d-2)$. For $d=2$, we recover the well-known result $M_c(d=2)=8\pi$ obtained within the standard Keller-Segel model (see [60] and references therein) and for $d=3$, the critical mass associated with the GKS model is $M_c(d=3)=202.8956\ldots$ (in usual dimensionless variables). This is similar to the Chandrasekhar limiting mass of white dwarf stars. The existence of a limiting mass for bacterial populations at the critical index n_3 and its connection to the Chandrasekhar mass was pointed out in [59,61] (and implicitly in [51]). This is another illustration of the numerous analogies that exist between self-gravitating systems and bacterial populations [53].

The paper is organized as follows. In Sec. II, we briefly recall the connection between white dwarf stars and gaseous polytropes. In Sec. III, we recall the basic properties of the SP and GSP systems and describe the behavior of the solutions depending on the index n and the dimension of space d. As the problem is very rich, involving many different cases ($\sim$30), a summary of previously obtained results, completed by new results and discussion, is required to understand the place of the present study in the general problem (see also Tables I and II for an overview). Then, we consider more specifically the particular index $n=n_3$ which presents a critical dynamics that was mentioned, but not studied, in our previous paper [51]. In Sec. IV, we show that this critical value can be understood from a simple dimensional analysis. In Sec. V, we study the critical collapse dynamics and extend the results obtained in $d=2$ for isothermal ($n=+\infty$) systems [12] to the case of *critical polytropes* ($n=n_3$) in $d>2$. In Sec. VI, we study the evaporation dynamics in unbounded space. We show that for $n>n_3$, self-gravity becomes negligible for large times so that the evaporation is eventually controlled by the pure (anomalous) diffusion. For $n=n_3$, gravity remains relevant at any time so that there exists a self-similar solution for which all the terms of the GSP system scale the same way. Finally, in Sec. VII, we transpose our main results to the context of chemotaxis using notations and parameters adapted to this problem (this is to facilitate the comparison with the results obtained in mathematical biology).

Our numerical and analytical study was conducted in parallel to a mathematical work by Blanchet *et al.* [62] who obtained rigorous results for the critical dynamics of the GSP system and GKS model introduced in our paper [51]. These two independent studies have different motivations and use very different methods so they are complementary to each other.

II. WHITE DWARF STARS AND POLYTROPES

In this section, we briefly recall the connection between the maximum mass of white dwarf stars (Chandrasekhar's mass [58]) and the theory of self-gravitating polytropic spheres [18,19].

In simplest models of stellar structure, a white dwarf star can be viewed as a degenerate gas sphere in hydrostatic equilibrium. The pressure is entirely due to the quantum pressure of the electrons (resulting from Pauli's exclusion principle for fermions) while the density of the star is dominated by the mass of the protons. The condition of hydrostatic equilibrium coupled to the Poisson equation reads

$$\nabla P=-\rho\nabla\Phi,\quad \Delta\Phi=4\pi G\rho, \tag{1}$$

and the equation of state of a degenerate gas of relativistic fermions at $T=0$ can be written parametrically as follows [63]:

$$P=A_2 f(x),\quad \rho=Bx^3, \tag{2}$$

where

TABLE I. Summary of the different regimes of the GSP system in $d>2$ with references to the physical literature ([P]: present paper; [N]: not done). The case of negative indices is considered in [52]. The links to the mathematical literature are indicated in the main text. *Note:* for $(n=\infty, T>T_c)$ and for $(n_3<n<\infty, \Theta>\Theta_c)$ in a bounded domain, the system can either reach a metastable equilibrium state or collapse depending on a notion of basin of attraction (see [11] for more details).

Index	Temperature	Bounded domain	Unbounded domain
$n=\infty$	$T>T_c$	Metastable equilibrium state (local minimum of free energy): box-confined isothermal sphere [11,12,35]	Evaporation [16]: asymptotically free normal diffusion (gravity negligible)
	$T<T_c$	Self-similar collapse with $\alpha=2$ [11,12,35] followed by a self-similar post-collapse leading to the formation of a Dirac peak of mass M [13]	Collapse: precollapse and postcollapse as in a bounded domain [11,12,35]
$0<n<n_3$	$\Theta>\Theta_c$	Equilibrium state: box-confined (incomplete) polytrope [51]	Equilibrium state: complete polytrope (compact support) [51]
	$\Theta<\Theta_c$	Equilibrium state: complete polytrope (compact support) [51]	
$n_3<n<\infty$	$\Theta>\Theta_c$	Metastable equilibrium state (local minimum of free energy): box-confined polytropic sphere [51]	Evaporation [P]: asymptotically free anomalous diffusion (gravity negligible)
	$\Theta<\Theta_c$	Self-similar collapse with $\alpha=2n/(n-1)$ [51] followed by a postcollapse leading to the formation of a Dirac peak of mass M [N]	Collapse: precollapse and postcollapse as in a bounded domain [51]
$n=n_3$	$\Theta>\Theta_c$	Equilibrium state: box-confined (incomplete) polytrope [51]	Self-similar evaporation modified by self-gravity [P]
	$\Theta<\Theta_c$	Pseudo-self-similar collapse leading to a Dirac peak of mass $(\Theta/\Theta_c)^{d/2}M$+halo [P]. This is followed by a postcollapse leading to a Dirac peak of mass M [N]	Collapse [N]
	$\Theta=\Theta_c$	Infinite family of steady states [P]	Infinite family of steady states [P]

TABLE II. Summary of the different regimes of the GSP system in $d=2$. In $d=1$, the GSP system always relaxes towards a statistical equilibrium state so that there is no evaporation or collapse [12,23,60].

Index	Temperature	Bounded domain	Unbounded domain
$n=\infty$	$T>T_c$	Equilibrium state: analytical solution [12]	Self-similar evaporation modified by self-gravity [16]
	$T<T_c$	Pseudo-self-similar collapse leading to a Dirac peak of mass $(T/T_c)M$+halo [12,30]. This is followed by a postcollapse leading to a Dirac peak of mass M [N]	Collapse [N]
	$T=T_c$	Self-similar collapse leading to a Dirac peak of mass M with exponential growth of $\rho(0,t)$ [12,47]	Self-similar collapse leading to a Dirac peak of mass M with logarithmic growth of $\rho(0,t)$ [16]
$0<n<\infty$	$T>T_c$	Equilibrium state: box-confined (incomplete) polytrope [51]	Equilibrium state: complete polytrope (compact support) [51]
	$T\leqslant T_c$	Equilibrium state: complete polytrope (compact support) [51]	

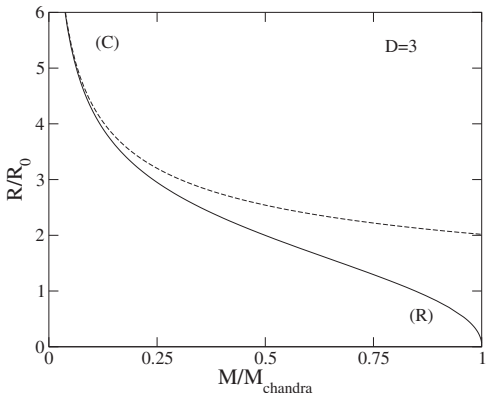

FIG. 1. Mass-radius relation for relativistic white dwarf stars at $T=0$ [58]. The radius vanishes for a limiting mass $M_{Chandra}$ corresponding to the ultrarelativistic limit (R). The dashed line corresponds to the classical limit (C).

$$A_2 = \frac{\pi m^4 c^5}{3h^3}, \quad B = \frac{8\pi m^3 c^3 \mu H}{3h^3}, \tag{3}$$

$$f(x) = x(2x^2 - 3)(1 + x^2)^{1/2} + 3\,\sinh^{-1} x, \tag{4}$$

where m is the mass of the electrons, H is the mass of the protons, and μ is the molecular weight. The function $f(x)$ has the asymptotic behaviors $f(x) \simeq (8/5)x^5$ for $x \ll 1$ and $f(x) \simeq 2x^4$ for $x \gg 1$. The classical limit corresponds to $x \ll 1$ and the ultrarelativistic limit to $x \gg 1$. In these limits, the white dwarf star is equivalent to a polytropic gas sphere with an equation of state $P = K\rho^\gamma$. The index n of the polytrope is defined by $\gamma = 1 + 1/n$. In $d=3$ dimensions, polytropes are self-confined for $n < 5$ and they are stable (with respect to the Euler-Poisson system) for $n \leqslant 3$ (for $n=3$ they are marginally stable). The mass-radius relation is given by [19]

$$M^{(n-1)/n} R^{(3-n)/n} = \frac{K(1+n)}{G(4\pi)^{1/n}} \omega_n^{(n-1)/n}, \tag{5}$$

where ω_n is a constant (depending only on the index n of the polytrope) that can be expressed in terms of the solution of the Lane-Emden equation [18].

In the classical case $x \ll 1$, the equation of state takes the form

$$P = K_1 \rho^{5/3}, \tag{6}$$

with

$$K_1 = \frac{1}{5}\left(\frac{3}{8\pi}\right)^{2/3} \frac{h^2}{m(\mu H)^{5/3}}. \tag{7}$$

Therefore a classical white dwarf star is equivalent to a polytrope of index $n = 3/2$. The mass-radius relation is given by

$$M^{1/3} R = \frac{1}{2}\left(\frac{3}{32\pi^2}\right)^{2/3} \frac{h^2}{mG(\mu H)^{5/3}} \omega_{3/2}^{1/3}, \tag{8}$$

with $\omega_{3/2} = 132.3843\ldots$. It exhibits the familiar $MR^3 \sim 1$ scaling.

In the ultrarelativistic limit $x \gg 1$, the equation of state takes the form

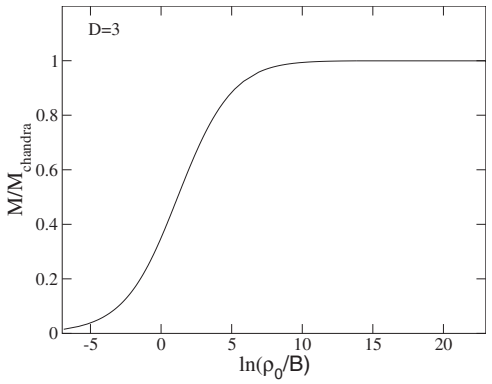

FIG. 2. Mass versus central density for relativistic white dwarf stars at $T=0$. Equilibrium states only exist for $M < M_{Chandra}$. For $M = M_{Chandra}$, the density profile is a Dirac peak. For $M > M_{Chandra}$, the system is expected to collapse and form a neutron star or a black hole. The corresponding density profiles are represented in Fig. 4 of [63].

$$P = K_2 \rho^{4/3}, \tag{9}$$

with

$$K_2 = \frac{1}{4}\left(\frac{3}{8\pi}\right)^{1/3} \frac{hc}{(\mu H)^{4/3}}. \tag{10}$$

Therefore, an ultrarelativistic white dwarf star is equivalent to a polytrope of index $n=3$. For this index, the relation (5) leads to a unique value of the mass

$$M_c = \left(\frac{3}{32\pi^2}\right)^{1/2} \omega_3 \left(\frac{hc}{G}\right)^{3/2} \frac{1}{(\mu H)^2}, \tag{11}$$

with $\omega_3 = 2.01824\ldots$. This is the Chandrasekhar mass

$$M_c = 0.196701\ldots \left(\frac{hc}{G}\right)^{3/2} \frac{1}{(\mu H)^2} \simeq 5.76 M_\odot/\mu^2. \tag{12}$$

Considering the general mass-radius relation of partially relativistic white dwarf stars (see Fig. 1), we note that, for this limiting value, the radius R of the configuration tends to zero. This leads to a Dirac peak with mass M_c. Thus, the Chandrasekhar mass represents the maximum mass of white dwarf stars (see Fig. 2). There is no hydrostatic equilibrium configuration for $M > M_c$.

If we extend Chandrasekhar's theory to a d-dimensional universe [61], we find that white dwarf stars become unstable in a universe with $d \geqslant 4$ dimensions [in $d=4$, classical white dwarf stars exist for a unique value of the mass $M = M_c = 0.014\,395\,8\ldots h^4/(m^2 G^2 \mu^3 H^3)$ and they are marginally stable]. Therefore, the dimension $d=3$ of our universe is very special regarding the laws of gravity. This is the largest dimension of space at which all the series of equilibria of white dwarf stars (from classical to ultrarelativistic) are stable. This may have implications regarding the anthropic principle.

III. SELF-GRAVITATING LANGEVIN PARTICLES

A. The generalized Smoluchowski-Poisson system

In this paper, we shall study a dynamical model of self-gravitating systems whose steady states reproduce the condi-

tion of hydrostatic equilibrium, Eq. (1). Specifically, we consider the generalized Smoluchowski-Poisson system [48]

$$\frac{\partial \rho}{\partial t} = \nabla \cdot \left[\frac{1}{\xi} (\nabla P + \rho \nabla \Phi) \right], \tag{13}$$

$$\Delta \Phi = S_d G \rho, \tag{14}$$

where $P(\rho)$ is a barotropic equation of state, i.e., the pressure $P(\mathbf{r},t)$ depends only on the density of particles $\rho(\mathbf{r},t)$. This model describes a *dissipative* gas of self-gravitating Langevin particles in an overdamped limit $\xi \to +\infty$ (where inertial effects are neglected) and in the thermodynamic limit $N \to +\infty$ (where the mean field approximation becomes exact) [17,64]. The GSP system is a particular example of generalized mean field Fokker-Planck equation [50]. It is associated to a stochastic process of the form

$$\frac{d\mathbf{r}}{dt} = -\frac{1}{\xi} \nabla \Phi + \sqrt{\frac{2P(\rho)}{\rho \xi}} \mathbf{R}(t), \tag{15}$$

where $\mathbf{R}(t)$ is a white noise with $\langle \mathbf{R}(t) \rangle = \mathbf{0}$ and $\langle R_i(t) R_j(t') \rangle = \delta_{ij} \delta(t-t')$. This stochastic process describes the evolution of each of the N Langevin particles interacting through the mean field potential $\Phi(\mathbf{r},t)$. For the sake of generality, we have allowed the strength of the noise term in Eq. (15) to depend on the local distribution of particles. This gives rise to anomalous diffusion and generalized pressure laws as discussed in [49,50].

The Lyapunov functional (or generalized free energy) associated with the GSP system is

$$F = \int \rho \int^{\rho} \frac{P(\rho')}{\rho'^2} d\rho' d\mathbf{r} + \frac{1}{2} \int \rho \Phi d\mathbf{r}. \tag{16}$$

Easy calculations lead to

$$\dot{F} = -\int \frac{\xi}{\rho} (\nabla P + \rho \nabla \Phi)^2 d\mathbf{r} \leqslant 0. \tag{17}$$

The GSP system has the following properties: (i) the total mass is conserved. (ii) $\dot{F} \leqslant 0$. (iii) $\dot{F} = 0 \Leftrightarrow \nabla P + \rho \nabla \Phi = \mathbf{0}$ (hydrostatic equilibrium) $\Leftrightarrow \partial_t \rho = 0$. (iv) $\rho_{eq}(\mathbf{r})$ is a steady state of the GSP system iff it is a critical point of $F[\rho]$ at fixed mass. (v) A steady state of the GSP system is linearly dynamically stable iff it is a (local) minimum of $F[\rho]$ at fixed mass [65]. By Lyapunov's direct method [49], we know that if $F[\rho]$ is bounded from below, the GSP system will relax towards a (local) minimum of $F[\rho]$ at fixed mass for $t \to +\infty$. If $F[\rho]$ has several minima, the choice of the selected minimum will depend on a notion of basin of attraction: if the initial condition is sufficiently "close" to the minimum $\rho_{eq}(\mathbf{r})$, the distribution $\rho(\mathbf{r},t)$ will converge towards $\rho_{eq}(\mathbf{r})$ for $t \to +\infty$. Finally, if $F[\rho]$ has no global minimum (as can be the case for self-gravitating systems), the system can either tend to a local minimum (metastable) if it exists, or undergo collapse or evaporation.

We are not claiming that this simple model accurately describes the dynamics of white dwarf stars or other astrophysical systems. However, we have undertaken a systematic study of the GSP system for different equations of state that have been considered in astrophysics. The main interest of this model is its simplicity (while being still very rich) which enables an accurate numerical and analytical treatment. This can be viewed as a first step before considering other, more realistic, dynamical models of self-gravitating systems. On the other hand, in a completely different context, this model is isomorphic to the standard Keller-Segel model describing the chemotaxis of bacterial populations (see Sec. VII). This is a further motivation to study this type of equations at a general level [67].

B. Isothermal spheres

For an isothermal equation of state $P = \rho k_B T/m$, we recover the standard Smoluchowski-Poisson system [11],

$$\frac{\partial \rho}{\partial t} = \nabla \cdot \left[\frac{1}{\xi} \left(\frac{k_B T}{m} \nabla \rho + \rho \nabla \Phi \right) \right], \tag{18}$$

$$\Delta \Phi = S_d G \rho. \tag{19}$$

Equation (18) is an ordinary mean field Fokker-Planck equation associated with a Langevin dynamics of the form

$$\frac{d\mathbf{r}}{dt} = -\frac{1}{\xi} \nabla \Phi + \sqrt{\frac{2k_B T}{\xi m}} \mathbf{R}(t), \tag{20}$$

where the strength of the noise is constant. The Lyapunov functional of the SP system can be written

$$F = k_B T \int \frac{\rho}{m} \ln \frac{\rho}{m} d\mathbf{r} + \frac{1}{2} \int \rho \Phi d\mathbf{r}. \tag{21}$$

This is the Boltzmann free energy $F_B = E - TS_B$, where $E = (1/2) \int \rho \Phi d\mathbf{r}$ is the energy and $S_B = -k_B \int (\rho/m) \ln(\rho/m) d\mathbf{r}$ is the Boltzmann entropy. The stationary solutions of the SP system are given by the Boltzmann distribution

$$\rho = A e^{-\beta m \Phi}, \tag{22}$$

where A is a constant determined by the mass M. These steady states can also be obtained by extremizing F at fixed mass, writing $\delta F - \alpha \delta M = 0$, where α is a Lagrange multiplier. The equilibrium distribution is obtained by substituting Eq. (22) into Eq. (19) leading to the Boltzmann-Poisson equation. Specializing on spherically symmetric distributions and defining

$$\rho = \rho_0 e^{-\psi(\xi)}, \quad \xi = r/r_0 = (S_d \beta G m \rho_0)^{1/2} r, \tag{23}$$

where ρ_0 is the central density, we find after simple algebra that ψ is solution of the Emden equation

$$\frac{1}{\xi^{d-1}} \frac{d}{d\xi} \left(\xi^{d-1} \frac{d\psi}{d\xi} \right) = e^{-\psi}, \tag{24}$$

with $\psi = 0$ and $\psi' = 0$ at $\xi = 0$. The Emden equation can also be obtained from the fundamental equation of hydrostatic equilibrium for an isothermal equation of state [12,18,19]. Note that the isothermal spheres have a self-similar structure $\rho(r)/\rho_0 = e^{-\psi(r/r_0)}$: if we rescale the central density and the radius appropriately, they have the same profile $e^{-\psi(\xi)}$. This property is called homology [19].

For $d=1$, the SP system is equivalent to the Burgers equation [23,60] and it relaxes towards the Camm distribution [68] which is a global minimum of free energy for any temperature. For $d>2$, there is no steady state with finite mass in an unbounded domain because the density of an isothermal self-gravitating system decreases as $\rho\sim r^{-2}$ for $r\to+\infty$ [19]. We shall thus enclose the system within a box of radius R [69]. For box-confined systems, we must integrate the Emden equation (24) until the normalized box radius $\xi=\alpha$ with

$$\alpha=(S_d\beta Gm\rho_0)^{1/2}R. \tag{25}$$

It is useful to define a dimensionless control parameter

$$\eta=\frac{\beta GMm}{R^{d-2}}. \tag{26}$$

Using the conservation of mass or the Gauss theorem, we obtain [12]

$$\eta=\alpha\psi'(\alpha). \tag{27}$$

This equation relates the central density to the mass and the temperature. More precisely, the relation $\eta(\alpha)$ gives the mass M as a function of the central density (for a fixed temperature T) or the temperature T as a function of the density contrast $\mathcal{R}\equiv\rho(0)/\rho(R)=e^{\psi(\alpha)}$ (for a fixed mass M). The curve $\eta(\alpha)$ is plotted in Fig. 3 of [12]. For $2<d<10$, the series of equilibria $\eta(\alpha)$ oscillates and presents a first turning point at $\eta_c=\eta(\alpha_1)$ (for $d\geqslant 10$, the series of equilibria does not display any oscillation). According to Poincaré's turning point argument [5,70], configurations with $\alpha>\alpha_1$ are unstable (saddle points of free energy at fixed mass). This concerns in particular the singular isothermal sphere corresponding to $\alpha\to+\infty$. Configurations with $\alpha<\alpha_1$ are metastable (local minima of free energy at fixed mass) and they exist only for $\eta\leqslant\eta_c$. There is no global minimum of free energy for self-gravitating isothermal spheres. For $\eta\leqslant\eta_c$, depending on the form of the initial density profile, the SP system can either relax towards a box-confined isothermal sphere (metastable) or collapse. This behavior has been illustrated numerically in Fig. 16 of [11]. For $\eta>\eta_c$ the SP system undergoes gravitational collapse. This self-similar collapse, followed by the formation of a Dirac peak, has been studied in detail in [12,13]. If we remove the box, the SP system can either collapse or evaporate depending on the initial condition (this behavior will be illustrated numerically in Sec. VI A).

The dimension $d=2$ is critical and has been studied in detail in [12,16]. The solution of the Emden equation is known analytically [71],

$$e^{-\psi}=\frac{1}{\left(1+\frac{1}{8}\xi^2\right)^2}. \tag{28}$$

In an unbounded domain, the density profile extends to infinity but the total mass is finite because the density decreases as r^{-4} for $r\to+\infty$. The total mass $M=\int_0^{+\infty}\rho 2\pi r dr$ is given by

$$M=\frac{1}{\beta Gm}\int_0^{+\infty}e^{-\psi}\xi d\xi=\frac{1}{\beta Gm}\lim_{\xi\to+\infty}\xi\psi'(\xi), \tag{29}$$

where we have used the Emden equation (24) to obtain the last equality. Using Eq. (28), we find that $\xi\psi'\to 4$ for $\xi\to+\infty$. This yields a unique value of the mass (for a fixed temperature), or equivalently a unique value of the temperature (for a fixed mass) given by

$$M_c=\frac{4k_BT}{Gm},\quad k_BT_c=\frac{GMm}{4}. \tag{30}$$

For $T=T_c$ or $M=M_c$, we have an infinite family of steady states

$$\rho(r)=\frac{\rho_0}{\left(1+\frac{1}{8}(r/r_0)^2\right)^2},\quad \rho_0r_0^2=\frac{k_BT}{2\pi Gm}, \tag{31}$$

parametrized by the central density ρ_0. For $\rho_0\to+\infty$, we obtain a Dirac peak with mass M_c. The steady states (31) have the same value of the free energy, independently on the central density ρ_0 (see Appendix A) and they are marginally stable ($\delta^2F=0$). For $T\neq T_c$ or $M\neq M_c$, there is no steady state in an infinite domain. For $T>T_c$ or $M<M_c$, the solution of the SP system evaporates and for $T<T_c$ or $M>M_c$, the solution of the SP system collapses. These different regimes have been discussed in detail in [12,16].

If we consider box confined configurations in $d=2$, we observe that the control parameter (26) is independent on the box radius and can be written

$$\eta=\beta GMm=4\frac{M}{M_c}=4\frac{T_c}{T}. \tag{32}$$

Using Eqs. (27) and (28), we obtain the relation $\eta(\alpha)=(\alpha^2/2)/(1+\alpha^2/8)$ between the central density, the mass, and the temperature. The density profiles are given by Eq. (31) with $8(r_0/R)^2=(T/T_c-1)=(M_c/M-1)$ so the central density is now determined by the mass M or the temperature T. Equilibrium states exist only for $\eta\leqslant\eta_c=4$, i.e., $M\leqslant M_c$ or $T\geqslant T_c$ and, since the series of equilibria is monotonic, they are fully stable (global minima of free energy at fixed mass). In that case, the SP system tends to a box-confined isothermal sphere. For $\eta=\eta_c=4$, i.e., $M=M_c$ or $T=T_c$, the steady state is a Dirac peak containing all the mass. For $\eta>\eta_c=4$ the SP system undergoes gravitational collapse (see Sec. V).

The mass-central density (for a fixed temperature) of two-dimensional isothermal spheres is plotted in Fig. 3. We note the striking analogy with the mass-central density of white dwarf stars in Fig. 2. Therefore, the critical mass (30) of isothermal spheres in two dimensions shares some resemblance with the Chandrasekhar mass. We shall show in the next section that this analogy (which is not obvious *a priori*) bears more significance than is apparent at first sight.

C. Complete polytropes

If we consider a polytropic equation of state $P=K\rho^\gamma$ with $\gamma=1+1/n$, we obtain the polytropic Smoluchowski-Poisson system [51]

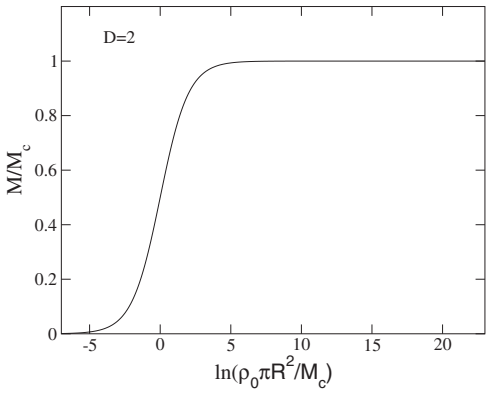

FIG. 3. Mass as a function of the central density for two-dimensional box-confined self-gravitating isothermal spheres with fixed temperature. Equilibrium states exist only for $M \leqslant M_c$. For $M=M_c$, the density profile is a Dirac peak and for $M>M_c$ the system undergoes gravitational collapse. More precisely, this curve represents $\eta(\alpha)/4$ so it also gives the inverse temperature T_c/T as a function of the density contrast $\mathcal{R}=\rho_0/\rho(R)=\mathcal{R}(\alpha)$ for a fixed mass. The corresponding density profiles are represented in Fig. 1 of [60].

$$\frac{\partial \rho}{\partial t} = \nabla \cdot \left[\frac{1}{\xi} (K \nabla \rho^{\gamma} + \rho \nabla \Phi) \right], \tag{33}$$

$$\Delta \Phi = S_d G \rho. \tag{34}$$

Equation (33) is a generalized mean field Fokker-Planck equation associated with the stochastic process

$$\frac{d\mathbf{r}}{dt} = -\frac{1}{\xi} \nabla \Phi + \sqrt{\frac{2K}{\xi}} \rho^{(\gamma-1)/2} \mathbf{R}(t), \tag{35}$$

where the strength of the noise depends on the local density as a power law [72]. The Lyapunov functional of the polytropic SP system can be written

$$F = \frac{K}{\gamma - 1} \int (\rho^{\gamma} - \rho) d\mathbf{r} + \frac{1}{2} \int \rho \Phi d\mathbf{r}. \tag{36}$$

It can be interpreted as a generalized free energy of the form $F=E-T_{eff}S$ where $E=(1/2)\int \rho \Phi d\mathbf{r}$ is the energy, $T_{eff}=K$ is an effective temperature (polytropic temperature), and $S=-1/(\gamma-1)\int(\rho^{\gamma}-\rho)d\mathbf{r}$ is the Tsallis entropy (the polytropic index γ plays the role of the Tsallis q parameter). For $\gamma=1$, i.e., $n \to +\infty$, the polytropic equation of state $P=K\rho^{\gamma}$ reduces to $P=K\rho$. It coincides with an isothermal equation of state $P=\rho k_B T/m$ with temperature $K=k_B T/m$ leading to the standard Smoluchowski-Poisson system, Eqs. (18) and (19).

The stationary solutions of the GSP system (33) are given by the Tsallis distributions

$$\rho = \left[\lambda - \frac{\gamma - 1}{K\gamma} \Phi \right]_+^{1/(\gamma-1)}, \tag{37}$$

where λ is a constant determined by the mass M (by definition $[x]_+=x$ if $x \geqslant 0$ and $[x]_+=0$ if $x<0$). These steady states can also be obtained by extremizing F at fixed mass, writing $\delta F - \alpha \delta M = 0$, where α is a Lagrange multiplier. The equilibrium distribution is obtained by substituting Eq. (37) into Eq. (34) leading to the Tsallis-Poisson equation. Specializing on spherically symmetric solutions and defining

$$\rho = \rho_0 \theta^n(\xi), \quad \xi = r/r_0, \quad r_0 = \left[\frac{K(1+n)}{S_d G \rho_0^{1-1/n}} \right]^{1/2}, \tag{38}$$

where ρ_0 is the central density, we find after simple algebra that θ is solution of the Lane-Emden equation

$$\frac{1}{\xi^{d-1}} \frac{d}{d\xi} \left(\xi^{d-1} \frac{d\theta}{d\xi} \right) = -\theta^n, \tag{39}$$

with $\theta=1$ and $\theta'=0$ at $\xi=0$. The Lane-Emden equation can equivalently be derived from the fundamental equation of hydrostatic equilibrium with a polytropic equation of state [18,19,51]. Note that the polytropic spheres have a self-similar structure $\rho(r)/\rho_0=\theta^n(r/r_0)$: if we rescale the central density and the radius appropriately, they have the same profile $\theta^n(\xi)$. This property is called homology [19].

In this paper, we restrict ourselves to $n>0$. Let us first discuss the case $d>2$. For $n>n_5=(d+2)/(d-2)$, unbounded self-gravitating polytropes have infinite mass because their density profile decreases like $r^{-\alpha}$ for $r \to +\infty$, with $\alpha=2n/(n-1)$. For $n<n_5=(d+2)/(d-2)$, they are self-confined. In that case, the function θ vanishes at $\xi=\xi_1$ and the density vanishes at $R_*=r_0\xi_1$ which defines the radius of the polytrope. The relation between the radius and the central density is

$$R_* = \left[\frac{K(1+n)}{S_d G \rho_0^{1-1/n}} \right]^{1/2} \xi_1. \tag{40}$$

The total mass $M=\int_0^{R_*} \rho S_d r^{d-1} dr$ can be written as

$$M = S_d \rho_0 r_0^d \int_0^{\xi_1} \theta^n \xi^{d-1} d\xi = -S_d \rho_0 r_0^d \xi_1^{d-1} \theta_1', \tag{41}$$

where we have used the Lane-Emden equation (39) to obtain the last equality. Therefore, the relation between the mass and the central density is

$$M = -S_d \rho_0 \left[\frac{K(1+n)}{S_d G \rho_0^{1-1/n}} \right]^{d/2} \xi_1^{d-1} \theta_1'. \tag{42}$$

Eliminating the central density between Eqs. (40) and (42) and introducing the index

$$n_3 = \frac{d}{d-2}, \tag{43}$$

we obtain the mass-radius relation

$$M^{(n-1)/n} R_*^{[(d-2)(n_3-n)]/n} = \frac{K(1+n)}{G S_d^{1/n}} \omega_n^{(n-1)/n}, \tag{44}$$

where

$$\omega_n = -\xi_1^{(n+1)/(n-1)} \theta_1'. \tag{45}$$

Let us introduce the polytropic temperature

$$\Theta = \frac{K(1+n)}{nS_d^{1/n}}. \tag{46}$$

For $0<n<n_3$ there is one, and only one, steady state for each mass M and temperature Θ and it is fully stable (global minimum of F at fixed mass). The GSP system will relax towards this complete polytrope (note that for $n=1$ the radius R_* of the polytrope is independent on the mass). For $n_3<n<n_5$ there is one, and only one, steady state for each mass M and temperature Θ but it is unstable (saddle point of F at fixed mass). In that case, the system will either collapse or evaporate. The index n_3 is *critical*. For $n=n_3$, there exists steady solutions for a unique value of the mass (at fixed temperature Θ),

$$M_c = \left(\frac{n_3\Theta}{G}\right)^{n_3/(n_3-1)} \omega_{n_3}, \tag{47}$$

or for a unique temperature (at fixed mass M),

$$\Theta_c = \frac{G}{n_3}\left(\frac{M}{\omega_{n_3}}\right)^{(n_3-1)/n_3}. \tag{48}$$

For $d=3$, we have $M_c=(3\Theta/G)^{3/2}\omega_3=10.487\ldots(\Theta/G)^{3/2}$ and $\Theta_c=(G/3)(M/\omega_3)^{2/3}=0.208\,72\ldots(G/M)^{2/3}$. As we have seen in Sec. II, the Chandrasekhar limiting mass of relativistic white dwarf stars is connected to the limiting mass (47) of critical polytropes. For a polytropic equation of state with critical index $n=n_3$, and for $M=M_c$, we obtain an infinite family of steady solutions

$$\rho(r) = \rho_0\theta^{n_3}(r/r_0), \quad \rho_0 r_0^d = \frac{1}{S_d}\left(\frac{\Theta n_3}{G}\right)^{d/2}, \tag{49}$$

parametrized by the central density ρ_0. For $\rho_0\to+\infty$, the density profile tends to a Dirac peak with mass M_c. These solutions have the same equilibrium free energy $F[\rho_{eq}]=-dKM/(d-2)$ independently on the central density ρ_0 (see Appendix A) and they are marginally stable ($\delta^2F=0$). For $M<M_c$ (at fixed temperature) or $\Theta>\Theta_c$ (at fixed mass), the solutions of the GSP system evaporate and for $M>M_c$ (at fixed temperature) or $\Theta<\Theta_c$ (at fixed mass), they collapse. These different regimes will be studied in detail in Secs. V and VI.

For $d=2$, we find that $n_3\to+\infty$, so we realize that isothermal systems ($n=+\infty$) in two dimensions are similar to critical polytropes ($n=n_3$) in higher dimensions $d>2$. *This is why the critical mass of isothermal spheres in $d=2$ shares some analogies with the Chandrasekhar mass in $d=3$ since they both correspond to critical polytropes with index $n=n_3$* [61]. Comparing Eq. (29) with Eq. (41) we find that for $d\to2$ and $n=n_3\to+\infty$, we have the limit

$$\lim_{n_3\to+\infty} n_3\omega_{n_3} = 4. \tag{50}$$

This limit can also be obtained from Eq. (79) of [51]. With this relation, we find that the critical mass and the critical temperature in $d=2$ given by Eq. (30) are particular cases of Eqs. (47) and (48).

Finally, for $d=1$ with $n>0$ (and for $d=2$ with $0<n<+\infty$), the GSP system always relaxes towards a complete polytrope which is a global minimum of free energy. Thus there is no critical dynamics for $d<2$ (and for $d=2$ with $n\neq+\infty$).

D. Box confined polytropes

For systems confined within a box of radius R, we need to integrate the Lane-Emden equation (39) until the normalized box radius $\xi=\alpha$ with

$$\alpha = R/r_0 = \left[\frac{S_d G\rho_0^{1-1/n}}{K(n+1)}\right]^{1/2} R. \tag{51}$$

It is useful to define a dimensionless control parameter (the definition of this parameter has been slightly changed with respect to our previous paper [51]),

$$\eta = M\left[\frac{nS_d^{1/n}G}{K(1+n)}\right]^{n/(n-1)} \frac{1}{R^{(d-2)(n-n_3)/(n-1)}}. \tag{52}$$

In terms of the polytropic temperature (46), it can be rewritten

$$\eta = \frac{G^{n/(n-1)}M}{\Theta^{n/(n-1)}R^{(d-2)(n-n_3)/(n-1)}}. \tag{53}$$

Note that for $n\to+\infty$, we have $\Theta=K=k_BT/m$ and the definitions (26) and (53) coincide. Using the conservation of mass or the Gauss theorem, we obtain [51]

$$\eta = -n^{n/(n-1)}\alpha^{(n+1)/(n-1)}\theta'(\alpha), \quad \alpha<\xi_1. \tag{54}$$

This equation relates the central density to the mass (at fixed temperature and box radius). In fact, this relation is valid only for *incomplete polytropes* whose density profile is arrested by the box [i.e., $\rho(R)>0$]. For $n\geqslant n_5$, this is always the case. For $0<n<n_5$, using the identity

$$\frac{\alpha}{\xi_1} = \frac{R}{R_*}, \tag{55}$$

the polytrope is confined by the box if $R_*\geqslant R$, i.e., $\alpha\leqslant\xi_1$. For $R_*<R$, i.e., $\alpha>\xi_1$, we have *complete polytropes* whose density profile vanishes before the wall. In that case, we need to integrate the Lane-Emden equation until the natural polytropic radius $\xi=\xi_1$. For $\alpha>\xi_1$, the relation (54) is replaced by

$$\eta = n^{n/(n-1)}\omega_n\left(\frac{R_*}{R}\right)^{(d-2)(n-n_3)/(n-1)} \quad (\alpha>\xi_1), \tag{56}$$

which is equivalent to the mass-radius relation (44). Using Eq. (55), it can be expressed in terms of α, giving the relation between the mass and the central density (at fixed temperature) for complete polytropes. Finally, the intermediate case is $R_*=R$, i.e., $\alpha=\xi_1$, at which the density profile vanishes precisely at the box radius. In that case, we have

$$\eta = n^{n/(n-1)}\omega_n \quad (\alpha=\xi_1). \tag{57}$$

The relation $\eta(\alpha)$ defines the series of equilibria containing incomplete (for $\alpha<\xi_1$) and complete (for $\alpha>\xi_1$) polytropes. It gives the mass M as a function of the central density (for a fixed temperature Θ and box radius R) or

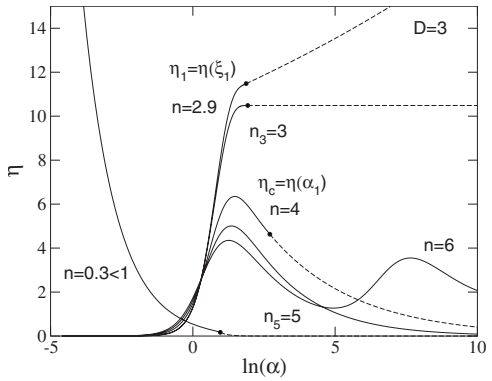

FIG. 4. Series of equilibria for box-confined polytropes with different index (the figure is done for $d=3$). The full lines ($\alpha<\xi_1$) correspond to incomplete polytropes whose profile is arrested by the box and the dashed lines ($\alpha>\xi_1$) correspond to complete polytropes that are self-confined.

the temperature Θ as a function of the density contrast $\mathcal{R}\equiv\rho_0/\rho(R)=\theta^{-n}(\alpha)$ (for a fixed mass M and radius R). Different examples of curves $\eta(\alpha)$ are represented in Fig. 4 for various indices in $d=3$.

(i) For $n<n_3$, the series of equilibria $\eta(\alpha)$ is monotonic. Since polytropic spheres are stable in absence of gravity (corresponding to $\alpha\to 0$) and since there is no turning point, the Poincaré argument implies that all the polytropes are stable. It can be shown furthermore that they are fully stable (global minima of free energy at fixed mass) so that the GSP system will tend to a steady state for $t\to+\infty$. For $\eta<\eta_1=\eta(\xi_1)=n^{n/(n-1)}\omega_n$, the GSP system tends to an incomplete polytrope confined by the box. For $\eta>\eta_1$, the GSP tends to a complete polytrope with radius $R_*<R$. This has been illustrated numerically in Fig. 21 of [51] for $n=3/2$ in $d=3$. This index corresponds to a classical white dwarf star in astrophysics. If we remove the box, the GSP system always tends to the complete polytrope.

(ii) For $n>n_3$, the series of equilibria $\eta(\alpha)$ presents a turning point at $\eta_c=\eta(\alpha_1)$. According to the Poincaré turning point argument, configurations with $\alpha>\alpha_1$ are unstable (saddle points of free energy at fixed mass). This concerns in particular the case of complete polytropes for $n_3<n<n_5$ (corresponding to $\alpha=\xi_1$), the Schuster polytrope $n=n_5$ and the singular polytropic spheres for $n\geqslant n_5$ (corresponding to $\alpha=+\infty$). Configurations with $\alpha<\alpha_1$ are metastable (local minima of free energy at fixed mass) and they exist only for $\eta\leqslant\eta_c$. There is no global minimum of free energy for $n>n_3$. For $\eta\leqslant\eta_c$, depending on the form of the initial density profile, the GSP system can either relax towards an incomplete polytrope confined by the box (metastable) or collapse. For $\eta>\eta_c$, the GSP system undergoes gravitational collapse. This self-similar collapse has been studied in detail in [51]. It is very similar to the self-similar collapse of isothermal systems in $d>2$ corresponding to $n\to+\infty$. If we remove the box, the GSP system can either collapse or evaporate depending on the initial condition (this will be illustrated numerically in Sec. VI).

(iii) The case $n=n_3$ is critical and will be studied in detail in this paper. For the critical index $n=n_3$, the control parameter is independent on the box radius and can be written

$$\eta=M\left(\frac{G}{\Theta}\right)^{n_3/(n_3-1)}. \tag{58}$$

In terms of the critical mass (47) or critical temperature (48), we have

$$\eta=n_3^{n_3/(n_3-1)}\omega_{n_3}\frac{M}{M_c}=n_3^{n_3/(n_3-1)}\omega_{n_3}\left(\frac{\Theta_c}{\Theta}\right)^{n_3/(n_3-1)}. \tag{59}$$

For incomplete polytropes with $\alpha<\xi_1$, the relation $\eta(\alpha)$ between the central density, the mass, and the temperature is given by Eq. (54). Their density profile is given by Eq. (49) where r_0 is determined by $(\Theta_c/\Theta)^{d/2}=M/M_c=-(1/\omega_{n_3})(R/r_0)^{d-1}\theta'(R/r_0)$, equivalent to relation (54), so the central density is now determined by the mass M or the temperature Θ. Complete polytropes with $\alpha\geqslant\xi_1$ exist for a unique value of the control parameter

$$\eta_c=n_3^{n_3/(n_3-1)}\omega_{n_3}. \tag{60}$$

This corresponds to the critical mass $M=M_c$ or critical temperature $\Theta=\Theta_c$. Equilibrium states exist only for $\eta\leqslant\eta_c$, i.e., $M\leqslant M_c$ or $\Theta\geqslant\Theta_c$. For $\eta<\eta_c$, they are fully stable (global minima of free energy at fixed mass). In that case, the GSP system relaxes towards an incomplete polytrope confined by the box. For $\eta=\eta_c$, i.e., $M=M_c$ or $\Theta=\Theta_c$, we have an infinite family of steady states parametrized by their central density $\alpha\geqslant\xi_1$ or equivalently by their radius $R_*\leqslant R$. They are marginally stable ($\delta^2F=0$). For $\eta>\eta_c$, i.e., $M>M_c$ or $\Theta<\Theta_c$, the GSP system undergoes gravitational collapse. The collapse dynamics is expected to be similar to the critical collapse of isothermal systems with $n\to+\infty$ in $d=2$ (see below). If we remove the box, the solution of the GSP system evaporates for $\eta<\eta_c$, i.e., $M<M_c$ or $\Theta>\Theta_c$ and collapses for $\eta>\eta_c$, i.e., for $M>M_c$ or $\Theta<\Theta_c$. These different regimes will be studied in detail in Secs. V and VI.

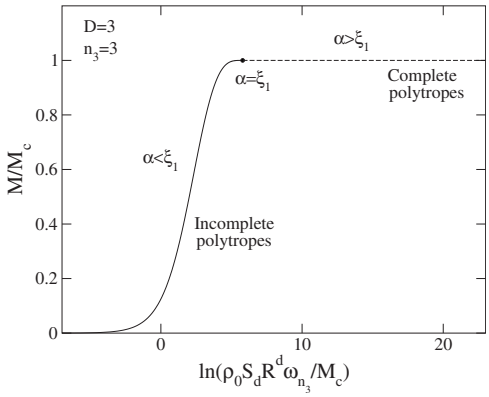

FIG. 5. Mass as a function of the central density for box-confined self-gravitating polytropic spheres with critical index $n=n_3=3$ in $d=3$. Incomplete polytropes with $\rho(R)>0$ are represented by a solid line and complete polytropes with $R_*\leqslant R$ are represented by a dashed line. For $\rho_0\to+\infty$, the density profile tends to a Dirac peak. Equilibrium states exist only for $M\leqslant M_c$. For $M>M_c$ the system undergoes gravitational collapse. The curve represents $\eta(\alpha)/[n_3^{n_3/(n_3-1)}\omega_{n_3}]$ so it also gives the inverse temperature $(\Theta_c/\Theta)^{n_3/(n_3-1)}$ as a function of the density contrast $\mathcal{R}(\alpha)$ for a fixed mass.

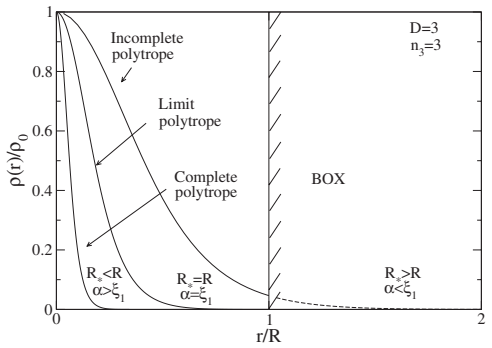

FIG. 6. Density profiles of complete and incomplete polytropes for the critical index $n_3=3$ in $d=3$. We have considered three values of the central density $\rho_0=(M_c/S_dR^d\omega_{n_3})\alpha^d$ corresponding to $\alpha=3<\xi_1$ (incomplete polytrope: $R_*>R$, $M<M_c$), $\alpha=\xi_1=6.896\,85\ldots$ (limit polytrope: $R_*=R$, $M=M_c$), and $\alpha=20>\xi_1$ (complete polytrope: $R_*<R$, $M=M_c$).

The mass-central density relation (for a fixed temperature) of box-confined self-gravitating polytropic spheres with critical index $n=n_3$ is plotted in Fig. 5 and the corresponding density profiles (illustrating the notion of complete and incomplete polytropes) are plotted in Fig. 6. We note the striking analogy with the mass-central density relation of white dwarf stars in Fig. 2. Indeed, ultrarelativistic white dwarf stars are equivalent to polytropes with critical index $n=n_3=3$ in $d=3$. In this context, the critical mass M_c corresponds to the Chandrasekhar limit. We emphasize, however, that we are considering here pure critical polytropes enclosed within a box while in Sec. II we considered self-confined *partially* relativistic white dwarf stars for which a box is not needed. It is only when $M\to M_{Chandra}$ (ultrarelativistic limit) that they become equivalent to pure polytropes. Furthermore, at $M=M_{Chandra}$ for white dwarf stars, the only steady state is a Dirac peak while at $M=M_c$ for pure critical polytropes, we have an infinite family of steady states with different central densities (the same difference holds between critical polytropes $n=n_3$ in $d>2$ and isothermal spheres $n=n_3=+\infty$ in $d=2$; compare Figs. 5 and 3). Finally, in Fig. 7, we plot the mass as a function of the central density for different dimensions of space d. This figure illustrates in particular the connection between the critical mass in $d=3$ reached for a finite value of the central density and the critical mass in $d=2$ reached for an infinite value of the central density.

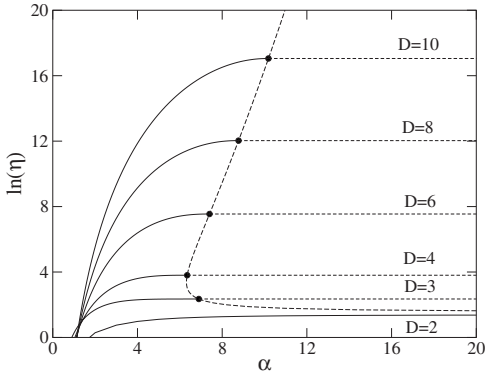

FIG. 7. Mass as a function of the central density for critical polytropes $n=n_3$ for different dimensions of space. We have plotted $\eta=n_3^{d/2}\omega_{n_3}M/M_c$ as a function of $\alpha=(\rho_0S_dR^d\omega_{n_3}/M_c)^{1/d}$. The maximum mass is reached at the bullet corresponding to $\alpha=\xi_1$, $\eta=\eta_c=n_3^{d/2}\omega_{n_3}$.

IV. THE CRITICAL INDEX FROM DIMENSIONAL ANALYSIS

It is instructive to understand the origin of the critical index $\gamma_{4/3}=2(d-1)/2$ or $n_3=d/(d-2)$ from simple dimensional analysis. Here we consider unconfined systems in d dimensions with arbitrary value of γ. The polytropic Smoluchowski-Poisson system can be written

$$\frac{\partial\rho}{\partial t}=\nabla\cdot\left[\frac{1}{\xi}(K\gamma\rho^{\gamma-1}\nabla\rho+\rho\nabla\Phi)\right]\equiv-\nabla\cdot\mathbf{J}, \quad (61)$$

$$\Delta\Phi=S_dG\rho. \quad (62)$$

The current $\mathbf{J}=\mathbf{J}_d+\mathbf{J}_g$ appearing in the Smoluchowski equation is the sum of two terms: a diffusion current $\mathbf{J}_d=-K\gamma\rho^{\gamma-1}\nabla\rho$ and a gravitational drift $\mathbf{J}_g=-\rho\nabla\Phi$. Based on dimensional analysis, the diffusion current can be estimated by

$$J_d\sim+K\gamma(M/L^d)^{\gamma-1}(\rho/L)\sim+(1/L)^{d(\gamma-1)+1}, \quad (63)$$

and the drift term by

$$J_g=-\rho GM/L^{d-1}\sim-(1/L)^{d-1}, \quad (64)$$

where M is the mass (constant) of the system and L is the characteristic size of the system.

The system will collapse to a point if gravity overcomes (anomalous) diffusion, i.e., $|J_g|\gg|J_d|$, when $L\to0$. This will be the case if $d-1>d(\gamma-1)+1$, i.e., $\gamma<\gamma_{4/3}$. Conversely, if $\gamma>\gamma_{4/3}$, the diffusion term can stabilize the system against gravitational collapse so that the system can be in stable equilibrium. The system will evaporate to infinity if (anomalous) diffusion overcomes gravity, i.e., $|J_d|\gg|J_g|$, when $L\to+\infty$. This will be the case if $d(\gamma-1)+1<d-1$, i.e., if $\gamma<\gamma_{4/3}$. Conversely, if $\gamma>\gamma_{4/3}$, the gravitational attraction can prevent evaporation so that the system can be in stable equilibrium. In conclusion, we find that the system can be in a stable equilibrium state iff $\gamma>\gamma_{4/3}$, i.e., $1/n>1/n_3$. In the opposite case, the system can either collapse to a point or evaporate to infinity. By this very simple argument, we recover the stability criterion of self-gravitating polytropic spheres obtained by other methods (see Appendix B of [61]).

The critical case is obtained when $J_d\sim J_g$, implying $d(\gamma-1)+1=d-1$, i.e., $\gamma=\gamma_{4/3}$ or, equivalently, $n=n_3$. In that case, the stability of the system will depend on its mass. The system will collapse to a point if gravity overcomes diffusion, i.e., $|J_g|\gg|J_d|$, when $L\to0$. This will be the case if $M>M_c$, where $M_c\sim(K/G)^{d/2}$ is a critical mass. The system will evaporate to infinity (in an unbounded domain) if (anomalous) diffusion overcomes gravity, i.e., $|J_d|\gg|J_g|$, when $L\to+\infty$. This will be the case if $M<M_c$. Therefore, at the critical index $\gamma=\gamma_{4/3}$, i.e., $n=n_3$, the system collapses if $M>M_c$ and evaporates if $M<M_c$. Again, this is fully consistent with the results obtained in Appendix B of [61].

V. COLLAPSE DYNAMICS

For $0<n<n_3$ in a space with $d\geqslant 2$ dimensions, the GSP system tends to an equilibrium state. For $n\geqslant n_3$, it can undergo gravitational collapse. For $n>n_3$ with $d>2$, the collapse is self-similar as studied in [51] (the case of negative indices $n<0$ is studied in [52]). In the present section, we consider the collapse dynamics of self-gravitating Langevin particles associated with the *critical* index $n_3=d/(d-2)$ in $d\geqslant 2$ dimensions which presents nontrivial features.

A. Generalities: Self-similar analysis

From now on, we adopt normalized variables such that $G=M=R=\xi=1$. The unique control parameter is the temperature Θ. For spherically symmetric solutions, using the Gauss theorem, the GSP system can be written in the form of an integrodifferential equation

$$\frac{\partial\rho}{\partial t}=\frac{1}{r^{d-1}}\frac{\partial}{\partial r}\left\{r^{d-1}\left[(S_d\rho)^{1/n}\Theta\frac{\partial\rho}{\partial r}+\frac{\rho}{r^{d-1}}\int_0^r\rho(r')S_d r'^{d-1}dr'\right]\right\}. \tag{65}$$

Introducing the mass within a sphere of radius r,

$$M(r,t)=\int_0^r\rho(r')S_d r'^{d-1}dr', \tag{66}$$

the GSP system can be formulated through a unique nonlinear dynamical equation for $M(r,t)$,

$$\frac{\partial M}{\partial t}=\Theta\left(\frac{1}{r^{d-1}}\frac{\partial M}{\partial r}\right)^{1/n}\left[\frac{\partial^2 M}{\partial r^2}-\frac{d-1}{r}\frac{\partial M}{\partial r}\right]+\frac{M}{r^{d-1}}\frac{\partial M}{\partial r}. \tag{67}$$

If the system of total mass $M=1$ is confined within a box of radius $R=1$, the appropriate boundary conditions are

$$M(0,t)=0,\quad M(1,t)=1. \tag{68}$$

If the system is not confined, the second condition should be replaced by

$$M(\infty,t)=1. \tag{69}$$

It is also convenient to introduce the function $s(r,t)=M(r,t)/r^d$ which has the same dimension as the density and which satisfies

$$\frac{\partial s}{\partial t}=\Theta\left(r\frac{\partial s}{\partial r}+ds\right)^{1/n}\left(\frac{\partial^2 s}{\partial r^2}+\frac{d+1}{r}\frac{\partial s}{\partial r}\right)+\left(r\frac{\partial s}{\partial r}+ds\right)s. \tag{70}$$

For $n\to+\infty$, these equations reduce to those studied in Refs. [11,12] in the isothermal case.

When the system collapses, it is natural to look for self-similar solutions of the form

$$\rho(r,t)=\rho_0(t)f\left(\frac{r}{r_0(t)}\right),\quad r_0=\left(\frac{\Theta}{\rho_0^{1-1/n}}\right)^{1/2}. \tag{71}$$

The relation between the core radius r_0 and ρ_0 (proportional to the central density [73]) is obtained by requiring that the diffusive term and the drift term in Eq. (65) scale in the same way. This relation can be rewritten $\rho_0 r_0^\alpha\sim 1$ with

$$\alpha=\frac{2n}{n-1}. \tag{72}$$

In terms of the mass profile, we have

$$M(r,t)=M_0(t)g\left(\frac{r}{r_0(t)}\right),\quad \text{with } M_0(t)=\rho_0 r_0^d, \tag{73}$$

and

$$g(x)=\int_0^x f(x')S_d x'^{d-1}dx'. \tag{74}$$

In terms of the function s, we have

$$s(r,t)=\rho_0(t)S\left(\frac{r}{r_0(t)}\right),\quad \text{with } S(x)=\frac{g(x)}{x^d}. \tag{75}$$

Inserting the ansatz (75) in Eq. (70) and using Eq. (71), we obtain

$$\frac{1}{\rho_0^2}\frac{d\rho_0}{dt}=\alpha, \tag{76}$$

and

$$\alpha S+xS'=(xS'+dS)^{1/n}\left(S''+\frac{d+1}{x}S'\right)+(xS'+dS)S. \tag{77}$$

Assuming that Eq. (77) has a solution so that the self-similar solution exists, Eq. (76) is readily integrated in

$$\rho_0(t)=\frac{1}{\alpha}(t_{coll}-t)^{-1}, \tag{78}$$

implying a finite time singularity. On the other hand, the invariant profile has the asymptotic behavior $f(x)\sim x^{-\alpha}$ for $x\to+\infty$.

B. The two-dimensional isothermal case

In $d=2$ dimensions, the critical index is $n_3=+\infty$ corresponding to the isothermal case studied in [12] (in that case $\Theta=T$). Since the study of the critical dynamics is rather complicated, it can be useful to summarize our results, with some complements and amplifications, before treating the case $d>2$.

In $d=2$, there exists a critical temperature $T_c=1/4$. If the system is enclosed within a box and $T>T_c$, it relaxes to an equilibrium distribution confined by the box. If the system is not confined and $T>T_c$, an evaporation process develops which has been studied in [16]. For $T=T_c$, the system undergoes gravitational collapse. The evolution is self-similar and leads to a Dirac peak containing the whole mass $M=1$ for $t\to+\infty$. In a bounded domain, the central density grows exponentially [12] rapidly with time and in an unbounded domain, the central density increases logarithmically [16] with time (and a tiny fraction of mass is ejected at large distances

to satisfy the moment of inertia constraint at $T=T_c$). Note that the Dirac peak is also the stationary solution of the SP system at $T=T_c$.

For $T<T_c$, and irrespective of the presence of a confining box, there is no steady state and the system collapses. Looking for an exact self-similar solution of the form (71) we obtain $\rho_0 r_0^2=T$, $\alpha=2=d$, and a scaling equation

$$\left(S''+\frac{3}{x}S'\right)+(xS'+2S)(S-1)=0. \tag{79}$$

However, this equation does not have any physical solution for large x. In fact, this could have been anticipated from the fact that the scaling functions $s(x)$ and $f(x)$ should decay as $x^{-2}=x^{-d}$ for large x. Then, the total mass in the profile is of order $\rho_0 r_0^2\int^{1/r_0}x^{-2}xdx\sim\ln(1/r_0)$, which unphysically diverges when r_0 goes to zero. Said differently, the scaling profile at $t=t_{coll}$ is $\rho\propto r^{-2}$ so that the mass $M=\int\rho(r)2\pi rdr$ diverges logarithmically for $r\to 0$. This logarithmic divergence is symptomatic of the formation of a Dirac peak resulting from a pseudo-self-similar collapse. In the case $d=2$, this situation can be analyzed analytically in great detail.

To that purpose, we note that the profile which cancels out the right-hand side of the SP system is exactly given by

$$M_1(r,t)=4T\frac{[r/r_0(t)]^2}{1+[r/r_0(t)]^2}, \tag{80}$$

$$\rho_1(r,t)=\frac{4\rho_0(t)}{\pi}\frac{1}{\{1+[r/r_0(t)]^2\}^2}, \tag{81}$$

with

$$\rho_0(t)r_0(t)^2=T. \tag{82}$$

If we consider time independent solutions ($\partial\rho/\partial t=0$) and impose the conservation of mass, we recover the steady solutions which exist for $T\geqslant T_c$ in a bounded domain [in that case $r_0=(T/T_c-1)^{1/2}$] and only for $T=T_c$ in an infinite domain (in that case we obtain a family of distributions parametrized by r_0). However, in the present case, we consider the case $T<T_c$ and seek the temporal evolution of $\rho_0(t)$ and $r_0(t)$. We argue that the solution (81) gives the leading contribution of the density profile in the core. This profile contains a mass T/T_c. We expect that the collapse will lead to $\rho_0(t)\to+\infty$ and $r_0(t)\to 0$ for $t\to t_{coll}$ (finite time singularity). Then, we see that the profile (81) leads to a Dirac peak with mass T/T_c, i.e.,

$$\rho_1(\mathbf{r},t)\to\frac{T}{T_c}\delta(\mathbf{r}). \tag{83}$$

The excess of mass will be contained in the profile extending in the halo. Therefore, we look for solutions of the form

$$\rho(r,t)=\rho_1(r,t)+\rho_2(r,t)$$
$$=\rho_0(t)f_1[r/r_0(t)]+\rho_0(t)^{\alpha(t)/2}f_2[r/r_0(t)]. \tag{84}$$

The first component has a scaling behavior and dominates in the center of the collapse region. It leads to a Dirac peak containing a fraction $M_c=T/T_c$ of the total mass $M=1$ at $t=t_{coll}$. The second component obeys a pseudoscaling and

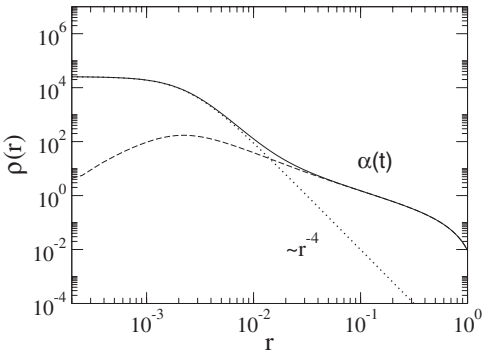

FIG. 8. For $d=2$, $n=n_3=+\infty$, and deep into the collapse regime for $T=T_c/2=1/8$, we plot the density profile (full line), emphasizing its two components: the core is dominated by the invariant scaling profile (dotted line) given analytically by Eq. (81) containing a mass $M_c=T/T_c$, and the halo obeys pseudoscaling (dashed line) with an exponent $\alpha(t)$ tending slowly to $d=2$ as $\rho_0\to+\infty$.

$f_2(x)\sim x^{-\alpha(t)}$ for large x, with an effective scaling exponent $\alpha(t)$ which very slowly approaches the value 2 (expected from the naive self-similar analysis) when $t\to t_{coll}$. Thus, at $t=t_{coll}$, we obtain

$$\rho(\mathbf{r},t)\to M_c\delta(\mathbf{r})+\chi(\mathbf{r},t), \tag{85}$$

where $\chi(r)$ is singular at $r=0$ behaving roughly as r^{-2}. In Fig. 8, we illustrate this decomposition of the density profile into two components. It is shown in [12] that the central density satisfies an equation of the form

$$\frac{1}{\rho_0}\frac{d\rho_0}{dt}\propto\rho_0^{\alpha(t)/2}, \tag{86}$$

instead of Eq. (76), and that the effective scaling exponent $\alpha(t)$ depends on the central density as

$$\epsilon(t)\equiv 1-\frac{\alpha(t)}{2}\sim\sqrt{\frac{\ln\ln\rho_0(t)}{2\ln\rho_0(t)}}. \tag{87}$$

This yields $\rho_0\sim(t_{coll}-t)^{-1+\epsilon(t)}$ or equivalently

$$\ln(\rho_0\tau)\sim-2\ln(r_0/\sqrt{\tau})\sim\sqrt{\frac{|\ln\tau|\ln|\ln\tau|}{2}}, \tag{88}$$

where we have noted $\tau=t_{coll}-t$.

Prior to our work [12], and unknown to us at that time, Herrero and Velazquez [30] had investigated the same problem in the context of chemotaxis using a different method based on match asymptotics. For $T<T_c$ (as far as we know, they did not consider the case $T=T_c$ treated in [12]), they showed that the system forms a Dirac peak of mass $M_c=T/T_c$ (within our notations) surrounded by a halo containing the excess of mass. On a qualitative point of view, the two scenarios are consistent. On a quantitative point of view, however, the scaling laws

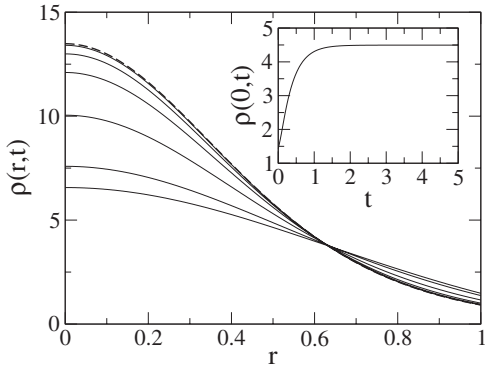

FIG. 9. In $d=3$ and for $n_3=3$ and $\Theta=0.25>\Theta_c$ in a finite box ($R=1$), we show the density at successive times, illustrating the convergence to the equilibrium density profile (dashed line). The inset illustrates the exponentially fast saturation of the central density for $\Theta>\Theta_c$, whereas a slower algebraic saturation is expected right at $\Theta=\Theta_c$.

$$\ln(\rho_0\tau) \sim -2\ln(r_0/\sqrt{\tau}) \sim \sqrt{2|\ln\tau|} + \frac{1}{2}\left(1-\frac{1}{\sqrt{|\ln\tau|}}\right)\ln|\ln\tau| \tag{89}$$

obtained by Herrero and Velazquez (HV) are slightly different from ours (SC). They lead to an effective exponent given by

$$1-\frac{\alpha(t)}{2} \sim \sqrt{\frac{2}{\ln\rho_0}} + \frac{1}{2}\left(1-\frac{1}{\sqrt{\ln\rho_0}}\right)\frac{\ln\ln\rho_0}{\ln\rho_0}, \tag{90}$$

instead of Eq. (87). For the densities accessible numerically, one obtains $\alpha_{SC}(\rho_0=10^3)=1.252\ldots$, while $\alpha_{HV}(\rho_0=10^3)=0.751\ldots$ and $\alpha_{SC}(\rho_0=10^5)=1.348\ldots$, while $\alpha_{HV}(\rho_0=10^5)=1.017\ldots$. Numerical simulations performed in [12] show a good agreement with the predicted values of α_{SC} for the accessible densities. However, in view of the complexity of the problem, and of the logarithmic (and sublogarithmic) corrections, it is difficult to understand the origin of the (slight) discrepancy between the two approaches. In any case, they both show that the collapse is not exactly self-similar but that the apparent scaling exponent $\alpha(t)$ is a very slowly varying function of the central density.

C. The critical polytropic case with $d>2$

We now consider the critical index $n=n_3=d/(d-2)$ with $d>2$. There exists a critical temperature $\Theta_c=1/[n_3\omega_{n_3}^{(n_3-1)/n_3}]$ (in $d=3$, we have $\Theta_c=0.208\,72\ldots$). If the system is confined within a box and $\Theta>\Theta_c$, it relaxes to an incomplete polytrope. This is illustrated in Fig. 9. If the system is not confined and $\Theta>\Theta_c$, an evaporation process develops which will be studied in the next section. In the confined case, when the generalized temperature Θ reaches the value Θ_c, the equilibrium density profile vanishes exactly at $R=1$. For $\Theta<\Theta_c$, and irrespective of the presence of a confining box, the system collapses.

We can naively look for self-similar solutions of the form described in Sec. V A. For $n=n_3$, we find $\alpha=d$, $\rho_0 r_0^d=\Theta^{d/2}$, and the scaling equation

$$S''+\frac{d+1}{x}S'+(xS'+dS)^{2/d}(S-1)=0. \tag{91}$$

It happens that as in the case ($d=2$, $n_3=\infty$), this equation does not have any physical solution for large x. Again, this could have been anticipated from the fact that the scaling functions $s(x)$ and $f(x)$ should decay as $x^{-2n_3/(n_3-1)}=x^{-d}$, for large x. Then, the total mass in the profile is of order

$$\rho_0 r_0^d \int^{1/r_0} x^{-d}x^{d-1}dx \sim \ln(1/r_0), \tag{92}$$

which unphysically diverges when r_0 goes to zero. Said differently, the scaling profile at $t=t_{coll}$ is $\rho\propto r^{-d}$ so that the mass $M=\int\rho(r)S_d r^{d-1}dr$ diverges logarithmically for $r\to 0$ [74].

Hence, for $n=n_3$ in $d>2$, we expect a situation similar to what was obtained for ($d=2$, $n_3=\infty$). However, the situation is more difficult to analyze because the stationary profile is not known analytically in the present case (this analytical profile was at the basis of our analysis in [12]). Using the results of Sec. III C, the profile which cancels out the right-hand side of the GSP system is given by

$$\rho_1(r,t)=\frac{n_3^{d/2}}{S_d}\rho_0(t)\theta_3^{n_3}[r/r_0(t)], \tag{93}$$

with

$$\rho_0(t)r_0(t)^d=\Theta^{d/2}. \tag{94}$$

If we consider time independent solutions ($\partial\rho/\partial t=0$) and impose the conservation of mass, we recover the steady solutions that exist for $\Theta\geqslant\Theta_c$ in a bounded domain [in that case, we have $(\Theta_c/\Theta)^{d/2}=-(1/\omega_{n_3})(R/r_0)^{d-1}\theta'(R/r_0)$] and only for $\Theta=\Theta_c$ in an infinite domain (in that case we obtain a family of distributions parametrized by r_0). However, in the present case, we consider the case $\Theta<\Theta_c$ and seek the temporal evolution of $\rho_0(t)$ and $r_0(t)$. We argue that the solution (93) gives the leading contribution of the density profile in the core. This profile vanishes at $R_*(r)=\xi_1 r_0(t)$, has a central density $(n_3^{d/2}/S_d)\rho_0(t)$, and contains a mass (see Sec. III C)

$$M_c=\left(\frac{\Theta}{\Theta_c}\right)^{d/2}. \tag{95}$$

We expect that the collapse will lead to $\rho_0(t)\to+\infty$ and $r_0(t)\to 0$. Then, we see that the profile (93) tends to a Dirac peak with mass M_c, i.e.,

$$\rho_1(\mathbf{r},t)\to\left(\frac{\Theta}{\Theta_c}\right)^{d/2}\delta(\mathbf{r}). \tag{96}$$

The excess of mass will be contained in the profile extending in the halo. Therefore, we look for solutions of the form

$$\rho(r,t)=\rho_1(r,t)+\rho_2(r,t)$$
$$=\rho_0(t)f_1[r/r_0(t)]+\rho_0(t)^{\alpha(t)/d}f_2[r/r_0(t)]. \tag{97}$$

The first component [75] has a scaling behavior and dominates in the center of the collapse region. It leads to a Dirac peak containing a fraction $M_c=(\Theta/\Theta_c)^{d/2}$ of the total mass at

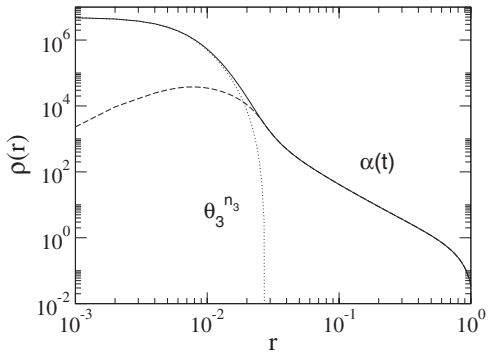

FIG. 10. For $d=3$, $n=n_3=3$, and deep into the collapse regime for $\Theta=0.75\Theta_c$, we plot the density profile (full line), emphasizing its two components: the core is dominated by the bounded invariant scaling profile (complete polytrope of index n_3) containing a mass $M_c=(\Theta/\Theta_c)^{3/2}$ (dotted line), and the halo obeys pseudoscaling (dashed line) with an exponent $\alpha(t)$ tending slowly to $d=3$ as $\rho_0 \to +\infty$.

$t=t_{coll}$. The second component obeys a pseudoscaling and $f_2(x) \sim x^{-\alpha(t)}$ for large x, with an effective scaling exponent $\alpha(t)$ which very slowly approaches the value d (expected from the naive self-similar analysis) when $t \to t_{coll}$. At $t=t_{coll}$, the first component $\rho_1(r,t)$ tends to a Dirac peak at the origin containing the mass M_c, whereas the second component develops a singularity at $r=0$. Thus, we have

$$\rho(\mathbf{r},t) \to M_c \delta(\mathbf{r}) + \chi(\mathbf{r},t), \tag{98}$$

with $\chi(r)$ behaving roughly as r^{-d}. In Fig. 10, we illustrate this decomposition of the density profile into two components.

In Fig. 11, we show that perfect scaling which would imply $\rho_0^{-1}(t)\frac{d\rho_0}{dt} \sim \rho_0$ is not obeyed. Instead, in the accessible density range, $\rho_0^{-1}(t)\frac{d\rho_0}{dt}$ decays with an apparent power law of ρ_0 which increases very slowly with time, but remains less than unity. We expect to have a relation of the form

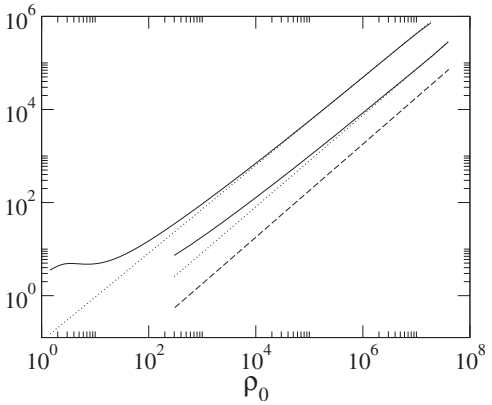

FIG. 11. For $\Theta=0.75\Theta_c$ (here $d=3$, $n=n_3=3$), we plot $\rho_0^{-1}(t)\frac{d\rho_0}{dt}$ (top full line) and $\hat{\rho}_0(t)$ (bottom full line) as a function of $\rho_0(t)$. Both grow with an effective exponent $\alpha/3 \approx 0.93$ (dotted lines), which slowly increases and should saturate to unity (the dashed line has slope unity).

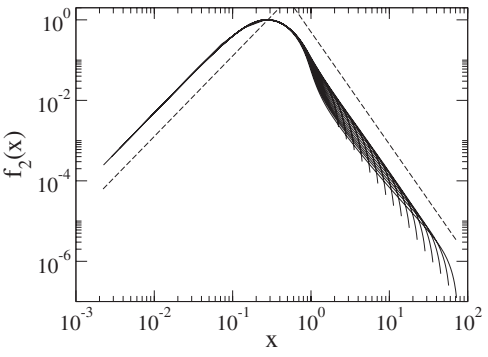

FIG. 12. For $\Theta=0.75\Theta_c$ (here $d=3$, $n=n_3=3$), we plot $f_2^{(\alpha)}(x)$ (as defined in the text) as a function of $x=r/r_0$, for different times for which the central density evolves from 10^2 to 10^7. Pseudoscaling is observed. The envelop of the tails decays with an apparent exponent $\alpha \approx 2.8$ (right dashed line), while the small x behavior is quadratic (left dashed line).

$$\frac{1}{\rho_0}\frac{d\rho_0}{dt} \propto \rho_0^{\alpha(t)/d}, \tag{99}$$

which is indeed confirmed by the numerics. In Fig. 11, we also plot the central density in the pseudoscaling component

$$\hat{\rho}_0(t) = \rho_0^{\alpha(t)/d}(t), \tag{100}$$

which shows that the effective exponent $\alpha(t)$ slowly converges to $\alpha=d$.

Finally in Fig. 12, we display the apparent scaling behavior of $\rho_2(r,t)=\rho_0(t)^{\alpha(t)/d} f_2[r/r_0(t)]$, associated to a value of $\alpha \approx 2.8$, fully compatible with the value obtained in Fig. 11 (in $d=3$).

VI. EVAPORATION DYNAMICS IN UNBOUNDED SPACE

A. The case $n > n_3$

When the system is not confined to a finite box, the nature of the dynamics crucially depends on the value of the polytropic index n with respect to n_3. As before, we consider $d \geqslant 2$ and $n>0$. If $n<n_3$, there exists equilibrium solutions (fully stable complete polytropes) which are reached for any initial density profile. If $n>n_3$, depending on the initial density profile and on the temperature, the system can collapse or evaporate. If R_0 is the typical extension of the initial density profile containing a mass M, one can form a quantity with the dimension of Θ:

$$\Theta_* = \frac{GM^{(n-1)/n}}{R_0^{(d-2)(n-n_3)/n}}, \tag{101}$$

which plays the role of an effective critical temperature. If $\Theta \ll \Theta_*$, the system should collapse as it would do if confined in a box of typical radius R_0 [51]. If $\Theta \gg \Theta_*$, the system should evaporate in the absence of an actual confining box. Hence, for a given initial profile, there exists a nonuniversal Θ_* separating these two regimes. We present numerical simulations for the case $n>n_3$. In Fig. 13, and for a particular initial process, we illustrate the fact that depending on the value of Θ with respect to a nonuniversal Θ_*, the

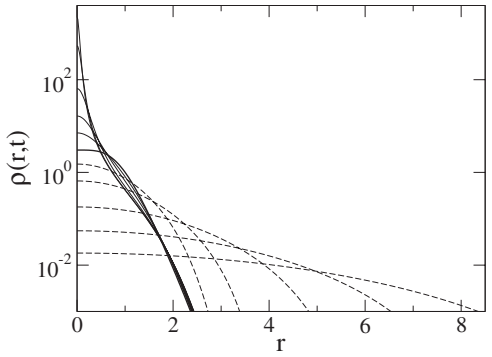

FIG. 13. In $d=3$ and $n=5>n_3$, and for a given initial density profile $[M(r)=r^3/(e^{-r^2}+r^2)^{3/2}$; thick line], we show the collapse dynamics observed at $\Theta=0.15$ (full lines for different times before t_{coll}) and the evaporation dynamics observed at $\Theta=1$ (dashed lines for different times). For this particular initial condition, we find $\Theta_* \approx 0.206$.

system can collapse or evaporate. In the evaporation regime and for $n>n_3$, a scaling analysis shows that gravity becomes gradually irrelevant and that this process becomes exclusively controlled by free (anomalous) diffusion. This fact is illustrated in Fig. 14. Indeed, when the evaporation length $r_0(t)\to+\infty$, we see from Eq. (67) that the gravitational term becomes negligible in front of the diffusion term,

$$\frac{M}{r^{d-1}}\frac{\partial M}{\partial r} \ll \Theta\left(\frac{1}{r^{d-1}}\frac{\partial M}{\partial r}\right)^{1/n}\frac{\partial^2 M}{\partial r^2}, \tag{102}$$

if $d>d/n+2$, i.e., $n>n_3$. Therefore, for $t\gg 1$, the GSP system reduces to the pure anomalous diffusion equation

$$\frac{\partial \rho}{\partial t} \simeq \frac{K}{r^{d-1}}\frac{\partial}{\partial r}\left(r^{d-1}\frac{\partial \rho^\gamma}{\partial r}\right), \tag{103}$$

with $K=S_d^{\gamma-1}\Theta/\gamma$. This equation has self-similar solutions that were discovered by Barenblatt [76] in the context of porous media. These solutions are closely related to the form of generalized thermodynamics introduced by Tsallis [56].

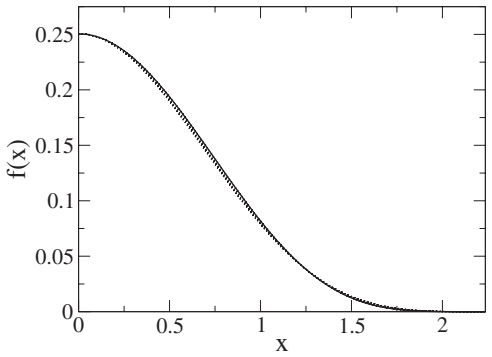

FIG. 14. In $d=3$ and $n=5>n_3$, we present the evaporation density data collapse at $\Theta=1$. As time proceeds, the effect of gravity becomes negligible, and the scaling profiles converge to the one corresponding to free diffusive evaporation (full line). This is the Barenblatt solution whose invariant profile is a Tsallis distribution of Eq. (114) with index γ.

Using the original idea of Plastino and Plastino [77], we look for solution of Eq. (103) in the form of a Tsallis distribution with index γ and time-dependent coefficients

$$\rho(r,t)=\frac{1}{Z}\rho_0(t)\{1-(\gamma-1)[r/r_0(t)]^2\}_+^{1/(\gamma-1)}. \tag{104}$$

For $\gamma>1$, i.e., $n>0$, we have a profile with compact support where the density vanishes at $r_{max}(t)=r_0(t)/\sqrt{\gamma-1}$. For $\gamma<1$, i.e., $n<0$, the density decreases like $\rho\sim r^{-2/(1-\gamma)}$ and the total mass is finite provided that $\gamma>\gamma_{1/3}\equiv(d-2)/d$, i.e., $n<-d/2$. Requiring that the profile (104) contains all the mass $M=1$, and imposing

$$\rho_0(t)r_0(t)^d=1, \tag{105}$$

we find the normalization factor

$$Z\equiv\int_0^{+\infty}[1-(\gamma-1)x^2]_+^{1/(\gamma-1)}S_d x^{d-1}dx. \tag{106}$$

Then, substituting the ansatz (104) with Eq. (105) in Eq. (103), we obtain

$$\dot{\rho}_0=-2dS_d^{\gamma-1}\Theta Z^{1-\gamma}\rho_0^{\gamma+2/d}. \tag{107}$$

Solving this equation with the initial condition $\rho(\mathbf{r},t=0)=\delta(\mathbf{r})$, we find that

$$\rho_0(t)=\frac{1}{[2d(\gamma-\gamma_{1/3})S_d^{\gamma-1}\Theta Z^{1-\gamma}t]^{1/(\gamma-\gamma_{1/3})}}. \tag{108}$$

This is valid for $\gamma>\gamma_{1/3}$, i.e., $n>0$ or $n<-d/2$. We note the scaling laws for large times,

$$\rho_0(t)\sim t^{-dn/(d+2n)},\quad r_0(t)\sim t^{n/(d+2n)}. \tag{109}$$

It is instructive to rederive this solution in a different manner, without presupposing the form of the solution. We look for general self-similar solutions of the form

$$\rho(r,t)=\rho_0(t)f[r/r_0(t)]. \tag{110}$$

We require that all the mass is in the profile (110) and impose the relation (105), implying that

$$\int_0^{+\infty}f(x)S_d x^{d-1}dx=1. \tag{111}$$

Substituting the ansatz (110) with Eq. (105) in Eq. (103), and imposing the condition (107) where Z is for the moment an arbitrary constant, we obtain the differential equation

$$\frac{1}{x^{d-1}}\frac{d}{dx}\left(x^{d-1}f^{\gamma-1}\frac{df}{dx}\right)=-2Z^{1-\gamma}(xf'+df). \tag{112}$$

Noting the identity $x^{d-1}(xf'+df)=(x^d f)'$, this equation can be integrated into

$$f^{\gamma-2}\frac{df}{dx}+2Z^{1-\gamma}x=0. \tag{113}$$

This first-order differential equation can again be readily integrated. We can choose the constant of integration so as to obtain a solution of the form

$$f(x) = \frac{1}{Z}[1-(\gamma-1)x^2]_+^{1/(\gamma-1)}. \quad (114)$$

Finally, the normalization condition (111) implies that Z is given by Eq. (106). It is interesting to realize that the q-exponential function $e_q(x)=[1+(q-1)x]_+^{1/(q-1)}$ introduced in the context of Tsallis generalized thermodynamics stems from the simple differential equation (113) related to the anomalous diffusion equation (103). Indeed, the scaling solution of this equation can be written

$$f(x) = \frac{1}{Z}e_\gamma(-x^2), \quad (115)$$

which generalizes the Gaussian distribution obtained for the ordinary diffusion equation recovered for $\gamma=1$. The moments $\langle r^k\rangle$ of the distribution (110) are given by

$$\langle r^k\rangle(t) = r_0(t)^k\int_0^{+\infty} f(x)x^{k+d-1}S_d dx. \quad (116)$$

They exist provided that $k>-d$ for $\gamma\geqslant 1$ and provided that $-d<k<2/(1-\gamma)-d$ for $\gamma<1$. They scale like $\langle r^k\rangle\propto r_0^k \propto t^{nk/(d+2n)}$.

The Tsallis entropy is finite for $\gamma>\gamma_{3/5}=d/(d+2)$ and it scales like

$$S(t)-nM = -n\rho_0^{1/n}\int_0^{+\infty} f(x)^\gamma S_d x^{d-1}dx \propto t^{-d/(d+2n)}. \quad (117)$$

On the other hand, for $d>2$, the potential energy $W=-1/(2S_d)\int(\nabla\Phi)^2 d\mathbf{r}$ scales like

$$W \propto \int_0^{+\infty}\left[\frac{M(r)}{r^{d-1}}\right]^2 r^{d-1}dr \propto \frac{1}{r_0^{d-2}} \propto t^{-n(d-2)/(d+2n)}. \quad (118)$$

Comparing Eqs. (117) and (118), we see that the potential energy is always negligible with respect to the entropy for $n>n_3$. Therefore, the Tsallis free energy behaves like

$$F(t)+nKM \propto t^{-d/(d+2n)}, \quad (119)$$

for $t\to+\infty$. Note that for $n_3<n<+\infty$, the free energy tends to a finite value $-nKM$ as the system spreads to infinity. Alternatively, for the isothermal case $n=+\infty$, the free energy is given by Eq. (95) of [16] and it tends to $-\infty$.

We can use the identity (B4) to derive the first correction in the evolution of the moments $\langle r^k\rangle$ due to self-gravity. To that purpose, we introduce the zeroth order solution (104) in the equation

$$\frac{d\langle r^k\rangle}{dt} = k(k+d-2)\int Pr^{k-2}d\mathbf{r} - k\int_0^{+\infty} r^{k-d}M(r)\frac{\partial M}{\partial r}dr. \quad (120)$$

The first term gives, after integration, the pure anomalous scaling

$$\langle r^k\rangle_0 \propto t^{nk/(d+2n)}. \quad (121)$$

The second term gives, after integration, the first correction due to gravity. If we write $\Delta\langle r^k\rangle=\langle r^k\rangle-\langle r^k\rangle_0$, we obtain

$$\Delta\langle r^k\rangle \propto t^{n(k-d)/d+2n+1}. \quad (122)$$

Let us consider some particular cases. (i) For $n\to+\infty$, we obtain $\Delta\langle r^k\rangle\propto t^{(k-d)/2+1}$. If we furthermore consider the second moment $k=2$ (moment of inertia), we recover the scaling $\Delta\langle r^2\rangle\propto t^{2-d/2}$ of [16]. (ii) For $k=d$, we find that $\Delta\langle r^d\rangle=-(d/2)t\propto t$ whatever the index n and the dimension of space d. (iii) For $n=n_3$, gravitational effects are of the same order as diffusive effects and $\langle r^k\rangle_0\propto\Delta\langle r^k\rangle\propto t^{k/d}$. This case will be studied in detail in the next section. (iv) Finally, let us introduce the number $k_0\equiv d-d/n-2$. For $k<k_0$, $\Delta\langle r^k\rangle\to 0$; for $k=k_0$, $\Delta\langle r^k\rangle\propto 1/t$; for $k>k_0$, $\Delta\langle r^k\rangle\to+\infty$.

B. The critical case $n=n_3$

Finally, for $n=n_3$, and since a critical Θ_c exists irrespective of the presence of a confining box, the system collapses for $\Theta<\Theta_c$ and evaporates for $\Theta>\Theta_c$. In the latter regime, gravity remains relevant and evaporation is controlled by both gravity and the diffusion process (see Fig. 15). Mathematically, this arises from the fact that there is an evaporation scaling solution for which all the terms of Eq. (65) scale in the same way. More specifically, we expect an evaporation density profile of the form

$$\rho(r,t) = \rho_0(t)f\left(\frac{r}{r_0(t)}\right), \quad \rho_0(t)r_0(t)^d = 1. \quad (123)$$

The relation between the evaporation length r_0 and ρ_0 (proportional to the central density) is obtained by requiring that the diffusive term and the drift term in Eq. (65) scale the same. In terms of the mass profile, we have

$$M(r,t) = g\left(\frac{r}{r_0(t)}\right) \quad \text{with } g(x) = \int_0^x f(x')S_d x'^{d-1}dx', \quad (124)$$

and in terms of the function s, we have

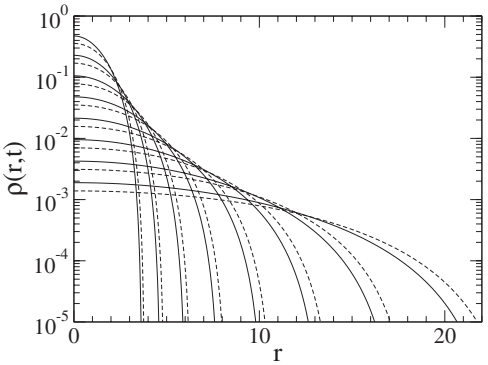

FIG. 15. In $d=3$ and for $n=n_3=3$, we compare the evaporation profiles at different times for $\Theta=1>\Theta_c$, for self-gravitating particles (full lines), to the faster evaporation dynamics when gravity is switched off (dashed lines).

$$s(r,t) = \rho_0(t) S\left(\frac{r}{r_0(t)}\right), \quad \text{with } S(x) = \frac{g(x)}{x^d}. \tag{125}$$

We require that all the mass is contained in the self-similar profile [78], which implies that

$$g(+\infty) = \int_0^{+\infty} f(x) S_d x^{d-1} dx = 1. \tag{126}$$

Inserting the ansatz (125) in Eq. (70), using Eq. (123), and imposing

$$\frac{1}{\rho_0^2}\frac{d\rho_0}{dt} = -d\Theta, \text{ i.e., } r_0^{d-1}\frac{dr_0}{dt} = \Theta, \tag{127}$$

we obtain the following scaling equation [note the change of sign compared to Eq. (77)] [79]:

$$S'' + \frac{d+1}{x}S' + (xS' + dS)^{2/d}\left(\frac{1}{\Theta}S + 1\right) = 0. \tag{128}$$

The evaporation radius is given by

$$r_0(t) = (d\Theta t)^{1/d}. \tag{129}$$

The moments scale like $\langle r^k \rangle \propto r_0^k \propto (d\Theta t)^{k/d}$ and the free energy scales like $F(t) + n_3 KM \propto t^{-(d-2)/d}$.

If we consider the large temperature limit $\Theta \gg 1$ where the diffusion term dominates on the gravitational drift, the foregoing differential equation reduces to

$$S'' + \frac{d+1}{x}S' + (xS' + dS)^{2/d} = 0. \tag{130}$$

In terms of the function f it can be written

$$f^{-2/d}f' + \frac{x}{S_d^{(d-2)/d}} = 0, \tag{131}$$

which is consistent with Eq. (113) up to the changes of notations in Eqs. (107) and (127). We can either solve this equation and impose the normalization condition (126) or make simple transformations in order to directly use the results of Sec. VI A. Indeed, let us set $\rho_0 = \sigma\rho_*$ and $r_0 = \mu r_*$. We impose $\rho_* r_*^d = 1$ leading to $\sigma\mu^d = 1$. On the other hand, we choose $\sigma = 2(S_d/Z)^{(d-2)/d}$ where Z is defined by Eq. (106) so that $\dot{\rho}_* = -2d(S_d/Z)^{(d-2)/d}\Theta\rho_*^2$. Then, $\rho = \rho_* f_*(r/r_*)$ with $f_*(x) = \sigma f(x/\mu)$. Now, ρ_*, r_*, and f_* have been defined so as to coincide with the functions ρ_0, r_0, and f of Sec. VI A. Thus, we obtain $f(x) = (1/\sigma) f_*(\mu x)$ where f_* is the function (114). Therefore, the normalized solution of Eq. (131) with the present notations can be written

$$f(x) = \frac{1}{\sigma Z}\left[1 - \frac{d-2}{d}\mu^2 x^2\right]_+^{d/(d-2)}, \tag{132}$$

with

$$\sigma\mu^d = 1, \quad \sigma = 2\left(\frac{S_d}{Z}\right)^{(d-2)/d}, \tag{133}$$

and where Z is given by Eq. (106). Proceeding along the lines of [16], we could expand the solutions of Eq. (128) (or of the equivalent equation for f) in powers of Θ^{-1} in the limit $\Theta \to +\infty$.

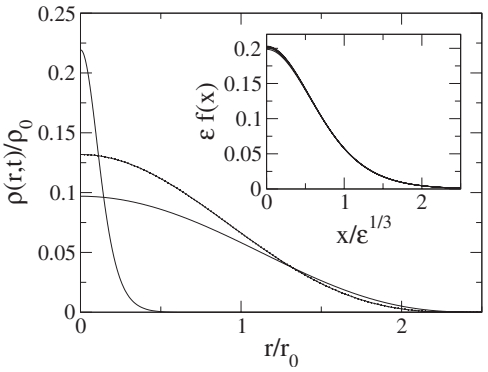

FIG. 16. In $d=3$ and for $n=n_3=3$, we compare the scaling profiles for $\Theta=0.21$ near $\Theta_c \approx 0.20872$, $\Theta=1$, and $\Theta=100$ (top to bottom full lines; for clarity, the $\Theta=0.21$ profile has been scaled down by a factor 150). For $\Theta \gg 1$, the invariant profile corresponds to the Barenblatt solution (pure anomalous diffusion) which is a Tsallis distribution with index $\gamma_{4/3} = 1 + 1/n_3$. For $\Theta \to \Theta_c$ the invariant profile tends to the profile of a steady polytrope with index n_3. For an intermediate temperature $\Theta=1$, we illustrate the perfect observed data collapse by plotting $r_0^d(t)\rho(r,t)$ as a function of $r/r_0(t)$, for $t=1.5^n (n=0,\ldots,13)$. These 14 curves are indistinguishable from the theoretical scaling profile. In the inset, we illustrate the scaling relation of Eq. (134) obtained for different values of $\varepsilon = (\Theta - \Theta_c)/\Theta_c \to 0$.

In Fig. 16, we show the form of the evaporation density profile f as a function of $\Theta > \Theta_c$. As Θ approaches Θ_c, the central density diverges, whereas the profile tends to the one corresponding to free diffusion for large Θ. In addition, we present numerical simulations for an intermediate Θ, showing that dynamical scaling is perfectly obeyed. Moreover, when $\Theta \to \Theta_c$, we find that the scaling function obeys itself a scaling relation (see inset of Fig. 16). Defining $\varepsilon = (\Theta - \Theta_c)/\Theta_c$, we find

$$f(\Theta, x) = \varepsilon^{-1} F(x/\varepsilon^{1/d}), \tag{134}$$

where F takes the form of a steady polytropic profile of index n_3. This scaling relation implies that close to Θ_c, the dth moment of r scales as

$$\langle r^d(t) \rangle \sim (\Theta - \Theta_c)t, \tag{135}$$

which is a generalization of our exact result for $d=2$ ($n_3 = +\infty$, $T_c = 1/4$) [16],

$$\langle r^2(t) \rangle = 4(T - T_c)t + \langle r^2(0) \rangle. \tag{136}$$

VII. ANALOGY BETWEEN THE LIMITING MASS OF WHITE DWARF STARS AND THE CRITICAL MASS OF BACTERIAL POPULATIONS

The generalized Smoluchowski-Poisson (GSP) system describing the dynamics of self-gravitating Langevin particles shares many analogies with the generalized Keller-Segel (GKS) model describing the chemotaxis of bacterial populations. Below, we briefly review the basic equations of chemotaxis and show the close link with the present work.

A. The generalized Keller-Segel model

The original Keller-Segel model has the form [20]

$$\frac{\partial \rho}{\partial t} = \nabla \cdot [D_2(\rho,c)\, \nabla\, \rho] - \nabla \cdot [D_1(\rho,c)\, \nabla\, c], \quad (137)$$

$$\epsilon \frac{\partial c}{\partial t} = -k(c)c + h(c)\rho + D_c \Delta c. \quad (138)$$

The drift-diffusion equation (137) governs the evolution of the density of bacteria $\rho(\mathbf{r},t)$ and the reaction-diffusion equation (138) governs the evolution of the secreted chemical $c(\mathbf{r},t)$. The bacteria diffuse with a diffusion coefficient D_2 and they also move in a direction of a positive gradient of the chemical (chemotactic drift). The coefficient D_1 is a measure of the strength of the influence of the chemical gradient on the flow of bacteria. On the other hand, the chemical is produced by the bacteria with a rate $h(c)$ and is degraded with a rate $k(c)$. It also diffuses with a diffusion coefficient D_c. In the primitive Keller-Segel model, $D_1=D_1(\rho,c)$ and $D_2=D_2(\rho,c)$ can both depend on the concentration of the bacteria and of the chemical. This can take into account microscopic constraints, such as close-packing effects [55,80,81] or anomalous diffusion [51].

If we assume a constant diffusion coefficient $D_2=D$ and a constant mobility $D_1/\rho=\chi$ (we also consider a constant production rate λ and a constant degradation rate k^2 of the chemical), we obtain the standard Keller-Segel (KS) model

$$\frac{\partial \rho}{\partial t} = \nabla \cdot (D\, \nabla\, \rho - \chi \rho\, \nabla\, c), \quad (139)$$

$$\epsilon \frac{\partial c}{\partial t} = \Delta c - k^2 c + \lambda \rho. \quad (140)$$

If we now assume that the diffusion coefficient and the mobility depend on the concentration of the bacteria, and if we set $D_2=Dh(\rho)$ and $D_1=\chi g(\rho)$, where h and g are positive functions, we obtain the generalized Keller-Segel (GKS) model [55,80,81],

$$\frac{\partial \rho}{\partial t} = \nabla \cdot [Dh(\rho)\, \nabla\, \rho - \chi g(\rho)\, \nabla\, c], \quad (141)$$

$$\epsilon \frac{\partial c}{\partial t} = \Delta c - k^2 c + \lambda \rho. \quad (142)$$

Equation (141) can be viewed as a nonlinear mean field Fokker-Planck (NFP) equation [50] associated with a stochastic process of the form

$$\frac{d\mathbf{r}}{dt} = \chi(\rho)\, \nabla\, c + \sqrt{2D(\rho)}\mathbf{R}(t), \quad (143)$$

with a diffusion coefficient $D(\rho)=(D/\rho)\int^{\rho} h(\rho')d\rho'$ and a mobility $\chi(\rho)=\chi g(\rho)/\rho$. These equations are associated with a notion of effective generalized thermodynamics [49,50]. The Lyapunov functional of the NFP equation Eqs. (141) and (142), can be written in the form of a generalized free energy $F=E-T_{eff}S$ where

$$E = \frac{1}{2\lambda}\int [(\nabla c)^2 + k^2 c^2] d\mathbf{r} - \int \rho c d\mathbf{r} \quad (144)$$

is the energy, $T_{eff}=D/\chi$ is an effective temperature given by an Einstein-like relation and

$$S = -\int C(\rho) d\mathbf{r}, \quad C''(\rho) = \frac{h(\rho)}{g(\rho)} \quad (145)$$

is a generalized entropy. A straightforward calculation shows that

$$\dot{F} = -\frac{1}{\lambda \epsilon}\int (-\Delta c + k^2 c - \lambda \rho)^2 d\mathbf{r} - \int \frac{1}{\chi g(\rho)} [Dh(\rho)\, \nabla\, \rho - \chi g(\rho)\, \nabla\, c]^2 d\mathbf{r} \leqslant 0, \quad (146)$$

which is the expression of the H theorem in the canonical ensemble adapted to dissipative systems. If we consider the particular case of a constant mobility $g(\rho)=\rho$ and a power-law diffusion $h(\rho)=\gamma\rho^{\gamma-1}$, with $\gamma=1+1/n$, we obtain the polytropic Keller-Segel model [51],

$$\frac{\partial \rho}{\partial t} = \nabla \cdot (D\, \nabla\, \rho^{\gamma} - \chi \rho\, \nabla\, c), \quad (147)$$

$$\epsilon \frac{\partial c}{\partial t} = \Delta c - k^2 c + \lambda \rho. \quad (148)$$

The standard Keller-Segel model is recovered for $\gamma=1$. Finally, if we neglect the degradation of the chemical ($k=0$) and consider a limit of large diffusivity of the chemical (implying $\epsilon=0$), we obtain for sufficiently large concentrations (see Appendix C of [81])

$$\frac{\partial \rho}{\partial t} = \nabla \cdot (D\, \nabla\, \rho^{\gamma} - \chi \rho\, \nabla\, c), \quad (149)$$

$$\Delta c = -\lambda \rho. \quad (150)$$

These equations are isomorphic to the generalized Smoluchowski-Poisson (GSP) system Eqs. (33) and (34), provided that we set

$$D = K/\xi, \quad \chi = 1/\xi, \quad c = -\Phi, \quad \lambda = S_d G. \quad (151)$$

Therefore, the results of the present paper apply to the chemotactic problem provided that the parameters are properly reinterpreted.

B. Formulation of the results with the biological variables

In the gravitational context, we usually fix the coefficients ξ, G, and M and use the temperature Θ as a control parameter. In the biological context, the coefficients D, χ, and λ are assumed given and the control parameter is the mass M. Therefore, it may be useful to briefly reformulate the previous results in terms of the mass, using notations adapted to the chemotactic problem.

For the critical index $n=n_3=d/(d-2)$ in $d\geqslant 2$, the steady states (polytropes) of the GKS model Eqs. (149) and (150) exist, in an unbounded domain, for a unique value of the mass given by [59]

$$M_c = S_d\left[\frac{D(1+n_3)}{\chi\lambda}\right]^{n_3/(n_3-1)}\omega_{n_3}. \quad (152)$$

For $d=3$, we have

$$M_c = 32\pi\omega_3\left(\frac{D}{\chi\lambda}\right)^{3/2} \simeq 202.8956\ldots\left(\frac{D}{\chi\lambda}\right)^{3/2}. \quad (153)$$

For $d=2$, using the identity (50), we recover the critical mass

$$M_c = \frac{8\pi D}{\chi\lambda}, \quad (154)$$

associated with the two-dimensional standard Keller-Segel (KS) model (see [60] and references therein). It is convenient to introduce rescaled variables so that $D=\lambda=\chi=1$. With this system of units the critical mass is $M_c(d)=S_d(1+n_3)^{n_3/(n_3-1)}\omega_{n_3}=S_d[2(d-1)/(d-2)]^{d/2}\omega_{d/(d-2)}$. For example, $M_c(d=2)=8\pi$ and $M_c(d=3)=32\pi\omega_3=202.8956\ldots$. Using the approximate expression of ω_n obtained in Eq. (B72) of [61], we can derive an approximate expression of the critical mass in the form

$$M_c^{approx}(d) = \frac{S_d}{d}[d(d+2)]^{d/2}. \quad (155)$$

For $d=2$, it returns the exact result $M_c^{approx}(2)=M_c=8\pi$. On the other hand, $M_c^{approx}(d=3)=243$ and $M_c^{approx}(d=4)=2842$. Using $S_d=2\pi^{d/2}/\Gamma(d/2)$ we find that $M_c^{approx}(d)\sim 2\pi^{d/2}d^d/\Gamma(d/2)$ for $d\to+\infty$.

Let us briefly discuss the critical dynamics of the GKS system with index $n=n_3=d/(d-2)$ for $d\geqslant 2$, depending on the total mass of the bacteria. For $M<M_c$, a box-confined system tends to an incomplete polytrope confined by the walls of the box. In an unbounded domain, the system evaporates in a self-similar way as discussed in Sec. VI B. For $M>M_c$, the system undergoes finite time collapse as discussed in Sec. V. In a finite time $t=t_{coll}$, it forms a Dirac peak containing a mass M_c surrounded by a collapsing halo evolving quasi-self-similarly with a time-dependent exponent $\alpha(t)$ tending extremely slowly to $\alpha=d$ as $t\to t_{coll}$. Thus,

$$\rho(\mathbf{r},t) \to M_c\delta(\mathbf{r}) + \chi(\mathbf{r},t), \quad (156)$$

where $\chi(r)$ behaves roughly as r^{-d} for $r\to 0$. For $M=M_c$, the situation is delicate and depends on the dimension of space. For $d=2$, in a bounded domain, the steady state of the KS model is a Dirac peak ($\rho_0=+\infty$). We have constructed in [12] a self-similar solution tending to this Dirac peak in infinite time. The central density increases exponentially rapidly. In an infinite domain, the KS model admits an infinite family of steady state solutions parameterized by their central density but the Dirac peak ($\rho_0=+\infty$) is selected dynamically (the other solutions have an infinite moment of inertia and, since the moment of inertia is conserved when $M=M_c$, they cannot be reached from an initial condition with a finite moment of inertia). We have constructed in [16] a self-similar solution tending to this Dirac peak in infinite time (and ejecting a small amount of mass at large distances so as to satisfy the moment of inertia constraint). The central density increases logarithmically rapidly. For $d>2$ and $M=M_c$, in a bounded domain, the GKS model admits an infinite family of steady state solutions parametrized by their central density or, equivalently, by their natural radius R_*. We have found numerically that the system tends to the polytrope where the density reaches zero at the box radius ($R_*=R$).

Due to the analogy between gravity and chemotaxis [53], we find that the critical mass of bacterial populations in the standard Keller-Segel model in $d=2$ and in the generalized Keller-Segel model in $d>2$ for the critical index $n=n_3$ shares some resemblance with the Chandrasekhar mass of white dwarf stars. For example, the curves of Figs. 3 and 5 also represent the mass of the bacterial aggregate as a function of the central density. As we have seen, they are strikingly similar to the mass-central density relation of white dwarf stars in Fig. 2. Therefore, bacteria and white dwarf stars share deep analogies despite their very different physical nature [59].

VIII. CONCLUSIONS AND PERSPECTIVES: THE GSP SYSTEM WITH A RELATIVISTIC EQUATION OF STATE

In this paper, we have studied the critical dynamics, at the index $n=n_3$, of the GSP system and GKS model describing self-gravitating Langevin particles and bacterial populations. This study completes our previous investigation [51] that was restricted to the cases $n<n_3$ and $n>n_3$. We have seen that, at the index $n=n_3$, there exists a critical mass M_c (independent on the size of the system) that is connected to the Chandrasekhar limiting mass of white dwarf stars [59]. In order to strengthen this analogy, it would be interesting to study the GSP system Eqs. (13) and (14), with the equation of state (2) corresponding to relativistic white dwarf stars. In fact, we can already describe qualitatively the behavior of the solutions by using the results obtained here for polytropes (see also the stability results obtained in [61] for relativistic white dwarf stars).

For $d=1$ and $d=2$, there exists an equilibrium state (global minimum of free energy) for all values of the mass M. Therefore, the GSP system relaxes towards that steady state.

For $d=3$, there exists a critical mass $M_{Chandra}=0.196\,701\ldots(hc/G)^{3/2}/(\mu H)^2$. For $M<M_{Chandra}$, the GSP system tends to a partially relativistic white dwarf star (global minimum of free energy). For $M\ll M_{Chandra}$, the density is small so that the equation of state reduces to that of a polytrope of index $n=3/2$ (classical limit). Therefore, the GSP system relaxes towards a classical white dwarf star as described in Fig. 21 of [51]. For $M=M_{Chandra}$ the density becomes large so that the equation of state reduces to that of a critical polytrope of index $n=3$ (ultrarelativistic limit). We expect that the GSP system forms a Dirac peak of mass $M_{Chandra}$ in infinite time. For $M>M_{Chandra}$, there is no equilibrium state and the system collapses. When the density reaches high values, the system becomes equivalent to a polytrope of index $n=3$. Therefore, according to the present

study, it forms in a finite time a Dirac peak of mass $M_{Chandra}$ surrounded by a halo evolving quasi-self-similarly with an exponent $\alpha(t)$ converging very slowly to $\alpha=3$.

For $d=4$, there exists a critical mass $M_c=0.014\,395\,8\ldots h^4/(m^2G^2\mu^3H^3)$ discovered in [61]. For $M<M_c$, the steady states are unstable and the system can either collapse or evaporate (depending on the form of the initial density profile and on the basin of attraction of the solution). In case of evaporation, when the density reaches low values, the system becomes equivalent to a polytrope of critical index $n_{3/2}=n_3=2$ (classical limit). In that case, it undergoes a self-similar evaporation similar to that described in Sec. VI B where diffusion and gravity scale the same way. In the case of collapse, when the density reaches high values, the system becomes equivalent to a polytrope of index $n_3'=4>n_3=2$ (ultrarelativistic limit). In that case, it undergoes a self-similar collapse similar to that described in [51]. For $M>M_c$, there is no steady state and the system collapses in the way discussed previously (energy considerations developed in [61] show that there is no evaporation in that case).

For $d\geqslant 5$, there is no steady state and the system can either collapse or evaporate. In case of evaporation, when the density reaches low values, the system becomes equivalent to a polytrope of index $n_{3/2}>n_3$. In that case, it undergoes a self-similar evaporation similar to that described in Sec. VI A where gravity becomes asymptotically negligible. In the case of collapse, when the density reaches high values, the system becomes equivalent to a polytrope of index $n_3'>n_3$. In that case, it undergoes a self-similar collapse similar to that described in [51].

As we have already mentioned, the real dynamics of white dwarf stars is not described by the GSP system, but is much more complicated. However, we think that the study of this simple dynamical model is an interesting first step before considering more complicated models. At least, it reveals the great richness of the problem. A next step would be to take into account inertial effects and study the (generalized) Kramers-Poisson system and the corresponding hydrodynamic equations [17].

APPENDIX A: VIRIAL THEOREM AND FREE ENERGY OF CRITICAL POLYTROPES

The scalar Virial theorem for the GSP system reads [16]

$$\frac{1}{2}\xi\frac{dI}{dt}=2E_{kin}+W_{ii}, \tag{A1}$$

where $I=\int\rho r^2 d\mathbf{r}$ is the moment of inertia, $E_{kin}=(d/2)\int P d\mathbf{r}$ is the kinetic energy of the microscopic motion, and $W_{ii}=-\int\rho\mathbf{r}\cdot\nabla\Phi d\mathbf{r}$ is the Virial. For $d=2$, $W_{ii}=-GM^2/2$ and for $d\neq 2$, $W_{ii}=(d-2)W$ where $W=(1/2)\int\rho\Phi d\mathbf{r}$ is the potential energy. If the system is enclosed within a box, we must add a term $-dP_b\mathrm{V}$ on the right-hand side, where P_b is the pressure against the box. In the following, we assume that the system is unbounded so that $P_b=0$.

For a polytropic equation of state $P=K\rho^\gamma$, with $\gamma=1+1/n$, the free energy (36) can be written

$$F=\frac{2n}{d}E_{kin}+W-nKM. \tag{A2}$$

Therefore, the Virial theorem can be expressed in the form

$$\frac{1}{2}\xi\frac{dI}{dt}=\frac{dF}{n}+W_{ii}-\frac{dW}{n}+dKM. \tag{A3}$$

For the critical index $n=n_3=d/(d-2)$, we obtain

$$\frac{1}{2}\xi\frac{dI}{dt}=(d-2)F+W_{ii}-(d-2)W+dKM. \tag{A4}$$

For $d\neq 2$, it reduces to

$$\frac{1}{2}\xi\frac{dI}{dt}=(d-2)F+dKM. \tag{A5}$$

For a steady state ($\dot{I}=0$), the Virial theorem implies

$$F_{eq}=-\frac{d}{d-2}KM. \tag{A6}$$

We have seen in Sec. III C that spherically symmetric steady states of the GSP system with $n=n_3$ exist for a unique value of the mass $M=M_c$ (for fixed K) or a unique value of the temperature $\Theta=\Theta_c$ (for fixed M) and form an infinite family of solutions parametrized by their central density ρ_0. According to Eq. (A6), they all have the same free energy, independent on the central density ρ_0. Therefore, thermodynamical arguments do not allow to select a particular solution among the whole family.

For $d=2$, the critical index $n_3\to+\infty$ and the equation of state is isothermal with $K=k_BT/m$. Then, the Virial theorem (A4) becomes [16]

$$\frac{1}{2}\xi\frac{dI}{dt}=2Nk_B(T-T_c), \tag{A7}$$

with $k_BT_c=GMm/4$. For a steady state ($\dot{I}=0$), the Virial theorem implies $T=T_c$ or $M=M_c$. It directly yields the result that unbounded two-dimensional isothermal spheres exist for a unique value of the mass or temperature. The spherically symmetric solution is given by Eq. (31) reading

$$\rho(r)=\frac{\rho_0}{[1+(\pi\rho_0/M)r^2]^2}. \tag{A8}$$

This family of steady solutions is parametrized by the central density ρ_0. The corresponding mass profile is given by $M(r)=\int_0^r\rho(r')2\pi r'dr$ and the gravitational potential can be obtained from the Gauss theorem $d\Phi/dr=GM(r)/r$ with the gauge condition $\Phi(r)\sim GM\ln r$ for $r\to+\infty$. This yields

$$M(r)=\frac{\pi\rho_0 r^2}{1+(\pi\rho_0/M)r^2}, \tag{A9}$$

$$\Phi(r)=\frac{GM}{2}\ln\left(\frac{M}{\pi\rho_0}+r^2\right). \tag{A10}$$

From these expressions, we find that the potential energy is

$$W = \frac{GM^2}{4}\left[1 + \ln\left(\frac{M}{\pi\rho_0}\right)\right]. \tag{A11}$$

On the other hand, the Boltzmann entropy $S_B = -k_B \int (\rho/m)\ln(\rho/m)d\mathbf{r}$ can be written

$$S_B = 2Nk_B\left[1 - \frac{1}{2}\ln\left(\frac{\rho_0}{m}\right)\right]. \tag{A12}$$

Therefore, the Boltzmann free energy $F_B = W - TS_B$ is given by

$$F_B = -\frac{GM^2}{4}\left[1 + \ln\left(\frac{\pi}{N}\right)\right]. \tag{A13}$$

We conclude that the free energy of unbounded isothermal spheres in two dimensions is independent on the central density ρ_0.

APPENDIX B: AN EQUATION FOR THE MOMENTS $\langle r^k \rangle$

Let us introduce the moments of order k:

$$I_k(t) = \int \rho r^k d\mathbf{r}. \tag{B1}$$

For $k=2$, we recover the moment of inertia. Taking the time derivative of Eq. (B1), using the generalized Smoluchowski equation (13) and integrating by parts, we obtain

$$\frac{1}{k}\xi\frac{dI_k}{dt} = -\int r^{k-2}\mathbf{r}\cdot\nabla P d\mathbf{r} - \int r^{k-2}\rho\mathbf{r}\cdot\nabla\Phi d\mathbf{r}. \tag{B2}$$

Integrating by parts the first term, we get

$$\frac{1}{k}\xi\frac{dI_k}{dt} = (k+d-2)\int P r^{k-2} d\mathbf{r} - \int r^{k-2}\rho\mathbf{r}\cdot\nabla\Phi d\mathbf{r}. \tag{B3}$$

If we take into account boundary effects, we need to introduce a pressure term $-\oint P r^{k-2}\mathbf{r}\cdot d\mathbf{S}$ on the right-hand side. For $k=2$, we recover the Virial theorem (A1). On the other hand, for a spherically symmetric system, using the Gauss theorem, the second integral can be simplified and we obtain

$$\frac{1}{k}\xi\frac{dI_k}{dt} = (k+d-2)\int P r^{k-2} d\mathbf{r} - G\int_0^{+\infty} r^{k-d} M(r)\frac{\partial M}{\partial r} dr. \tag{B4}$$

For $k=d$, the second integral can be calculated explicitly and we find

$$\frac{1}{d}\xi\frac{dI_d}{dt} = 2(d-1)\int P r^{d-2} d\mathbf{r} - \frac{GM^2}{2}. \tag{B5}$$

For $d=1$, the first term on the right-hand side must be replaced by $2P(0,t)$.

[1] V. A. Antonov, Vestn. Leningr. Univ., Ser. 4: Fiz., Khim. **7**, 135 (1962).
[2] D. Lynden-Bell, Bull. Astron. **3**, 305 (1968); D. Lynden-Bell and R. Wood, Mon. Not. R. Astron. Soc. **138**, 495 (1968).
[3] W. Thirring, Z. Phys. **235**, 339 (1970).
[4] T. Padmanabhan, Phys. Rep. **188**, 285 (1990).
[5] P. H. Chavanis, Int. J. Mod. Phys. B **20**, 3113 (2006).
[6] *Dynamics and Thermodynamics of Systems with Long Range Interactions*, edited by T. Dauxois *et al.*, Lecture Notes in Physics Vol. 602 (Springer, Berlin, 2002).
[7] *Dynamics and Thermodynamics of Systems with Long Range Interactions: Theory and Experiments*, edited by A. Campa *et al.*, AIP Conf. Proc. No. 970 (AIP, Melville, NY, 2008).
[8] A. I. Artemiev, I. E. Mazets, G. Kurizki, and D. O'Dell, Int. J. Mod. Phys. B **18**, 2027 (2004).
[9] P. Hertel and W. Thirring, in *Quanten und Felder*, edited by H. P. Dürr (Vieweg, Braunschweig, 1971).
[10] P. H. Chavanis, Phys. Rev. E **65**, 056123 (2002).
[11] P. H. Chavanis, C. Rosier, and C. Sire, Phys. Rev. E **66**, 036105 (2002).
[12] C. Sire and P. H. Chavanis, Phys. Rev. E **66**, 046133 (2002).
[13] C. Sire and P. H. Chavanis, Phys. Rev. E **69**, 066109 (2004).
[14] P. H. Chavanis and C. Sire, Phys. Rev. E **70**, 026115 (2004).
[15] J. Sopik, C. Sire, and P. H. Chavanis, Phys. Rev. E **72**, 026105 (2005).
[16] P. H. Chavanis and C. Sire, Phys. Rev. E **73**, 066103 (2006).
[17] P. H. Chavanis and C. Sire, Phys. Rev. E **73**, 066104 (2006).
[18] R. Emden, *Gaskugeln* (Teubner Verlag, Leipzig, 1907).
[19] S. Chandrasekhar, *An Introduction to the Theory of Stellar Structure* (Dover, New York, 1942).
[20] E. Keller and L. A. Segel, J. Theor. Biol. **26**, 399 (1970).
[21] W. Jager and S. Luckhaus, Trans. Am. Math. Soc. **329**, 819 (1992).
[22] J. D. Murray, *Mathematical Biology* (Springer, Berlin, 1991).
[23] L. Acedo, Europhys. Lett. **73**, 698 (2006).
[24] V. Nanjundiah, J. Theor. Biol. **42**, 63 (1973).
[25] S. Childress and J. K. Percus, Math. Biosci. **56**, 217 (1981).
[26] S. Childress, Lect. Notes Biomath. **55**, 61 (1984).
[27] T. Nagai, Adv. Math. Sci. Appl. **5**, 581 (1995).
[28] P. Biler, Stud. Math. **114**, 181 (1995).
[29] M. A. Herrero and J. J. L. Velazquez, Math. Ann. **306**, 583 (1996).
[30] M. A. Herrero and J. J. L. Velazquez, J. Math. Biol. **35**, 177 (1996).
[31] A. Stevens and H. G. Othmer, SIAM J. Appl. Math. **57**, 1044 (1997).
[32] M. A. Herrero, E. Medina, and J. L. Velazquez, Nonlinearity **10**, 1739 (1997).
[33] M. A. Herrero, E. Medina, and J. L. Velazquez, J. Comput. Appl. Math. **97**, 99 (1998).
[34] P. Biler, Adv. Math. Sci. Appl. **8**, 715 (1998).
[35] M. P. Brenner, P. Constantin, L. P. Kadanoff, A. Schenkel, and S. C. Venkataramani, Nonlinearity **12**, 1071 (1999).
[36] T. Nagai, J. Inequal. Appl. **6**, 37 (2001).
[37] C. Rosier, C. R. Acad. Sci., Ser. I: Math. **332**, 903 (2001).
[38] P. Biler and T. Nadzieja, Rep. Math. Phys. **52**, 205 (2003).

[39] D. Horstmann, Jahresber. Dtsch. Math.-Ver. **106**, 51 (2004).
[40] J. Dolbeault and B. Perthame, C. R. Acad. Sci., Ser. I: Math. **339**, 611 (2004).
[41] P. Biler, M. Cannone, I. A. Guerra, and G. Karch, Math. Ann. **330**, 693 (2004).
[42] L. Corrias, B. Perthame, and H. Zaag, Milan J. Math. **72**, 1 (2004).
[43] P. Biler, G. Karch, P. Laurençot, and T. Nadzieja, Topol. Methods Nonlinear Anal. **27**, 133 (2006).
[44] P. Biler, G. Karch, P. Laurençot, and T. Nadzieja, Math. Methods Appl. Sci. **29**, 1563 (2006).
[45] A. Blanchet, J. A. Carrillo, and N. Masmoudi, Commun. Pure Appl. Math. (to be published).
[46] A. Blanchet, J. Dolbeault, and B. Perthame, Electron. J. Differ. Equations **44**, 32 (2006).
[47] N. Kavallaris and P. Souplet, e-print arXiv:0804.4549.
[48] P. H. Chavanis, Phys. Rev. E **68**, 036108 (2003).
[49] T. D. Frank, *Nonlinear Fokker-Planck Equations* (Springer, Berlin, 2005).
[50] P. H. Chavanis, Eur. Phys. J. B **62**, 179 (2008).
[51] P. H. Chavanis and C. Sire, Phys. Rev. E **69**, 016116 (2004).
[52] P. H. Chavanis and C. Sire, Physica A **375**, 140 (2007).
[53] P. H. Chavanis, M. Ribot, C. Rosier, and C. Sire, Banach Cent Publ. **66**, 103 (2004).
[54] P. Biler, P. Laurençot, and T. Nadzieja, Adv. Differ. Equ. **9**, 563 (2004).
[55] P. H. Chavanis, Eur. Phys. J. B **54**, 525 (2006).
[56] C. Tsallis, J. Stat. Phys. **52**, 479 (1988).
[57] R. H. Fowler, Mon. Not. R. Astron. Soc. **87**, 114 (1926).
[58] S. Chandrasekhar, Astrophys. J. **74**, 81 (1931).
[59] P. H. Chavanis and C. Sire, Physica A **387**, 1999 (2008).
[60] P. H. Chavanis, Physica A **384**, 392 (2007).
[61] P. H. Chavanis, Phys. Rev. D **76**, 023004 (2007).
[62] A. Blanchet, J. A. Carrillo, and P. Laurençot (unpublished).
[63] S. Chandrasekhar, Mon. Not. R. Astron. Soc. **95**, 207 (1935).
[64] P. H. Chavanis, P. Laurençot, and M. Lemou, Physica A **341**, 145 (2004).
[65] Since the free energy $F[\rho]$ coincides with the energy functional $\mathcal{W}[\rho]$ of a barotropic gas (up to a positive macroscopic kinetic term) [66], we conclude that $\rho_{eq}(\mathbf{r})$ is linearly dynamically stable with respect to the GSP system iff it is formally nonlinearly dynamically stable with respect to the barotropic Euler-Poisson system [66].
[66] P. H. Chavanis, Astron. Astrophys. **451**, 109 (2006).
[67] We shall study the problem in d dimensions because (i) we have found that the structure of the mathematical problem with the dimension of space is very rich [12,51,61], exhibiting several characteristic dimensions. (ii) In gravity, the usual dimension is $d=3$ but, in biology (see Sec. VII), the bacteria (or cells) are compelled to lie on a plane so that $d=2$.
[68] G. L. Camm, Mon. Not. R. Astron. Soc. **110**, 305 (1950).
[69] It may appear artificial to put the system in a "box." In gravity, the box delimitates the region of space where the system can be assumed isolated from the surrounding and where statistical mechanics applies. In biology (see Sec. VII), the box has a physical meaning since it represents the container in which the bacteria (or cells) are confined.
[70] J. Katz, Found. Phys. **33**, 223 (2003).
[71] J. Ostriker, Astrophys. J. **140**, 10560 (1964).
[72] L. Borland, Phys. Rev. E **57**, 6634 (1998).
[73] The reader should be aware that, in the sections dealing with the dynamics, ρ_0 and r_0 do not exactly coincide with the quantities of the same name introduced in the sections dealing with the statics (they usually differ by a factor of proportionality).
[74] More generally, for a polytrope of index n we have $\rho \propto r^{-\alpha}$ at $t=t_{coll}$, with $\alpha=2n/(n-1)$ so that the self-similar solution exists provided that $\alpha-d+1<1$ leading to $1/n<1/n_3$ (i.e., $n>n_3$ for $d>2$). This is precisely the range of indices for which the complete polytropes are dynamically unstable [51].
[75] Defining $\rho_c(x)$ as the equilibrium density profile at $\Theta=\Theta_c$, then the first component can be written $\rho_1(r,t)=\frac{M_c}{r_0^d}\rho_c(r/r_0)$.
[76] G. I. Barenblatt, V. M. Entov, and V. M. Ryzhik, *Theory of Fluid Flows through Natural Rocks* (Kluwer Academic, Dordrecht, 1990).
[77] A. R. Plastino and A. Plastino, Physica A **222**, 347 (1995).
[78] Looking for a self-similar solution of the form (71) for any index n and requiring that the diffusion and gravity scale the same, we find that $\rho_0 r_0^{\alpha} \sim 1$ where α is given by Eq. (72). The profile will contain all the mass provided that $\rho_0 r_0^d \sim 1$ which implies $\alpha=d$ leading to $n=n_3$. Thus, it is only for the critical index that we can have a self-similar solution where the diffusion and gravity scale the same and which contains all the mass.
[79] The scaling equations (77) and (128) have a very different mathematical structure. The scaling equation for collapse (77), valid for $n>n_3$, leads to an eigenvalue problem for $S(x)$ [12,51]. Indeed, it admits a physical solution for a unique value of $S(0)$ equal to S_* (say). For $S(0)<S_*$, the solution becomes negative at some point, and for $S(0)>S_*$, it diverges at a finite x_0. By contrast, the scaling equation for evaporation (128), valid for $n=n_3$, admits a one parameter family of solutions parametrized by $S(0)$. Then, the suitable value S_* is selected by the normalization condition (126).
[80] T. Hillen and K. Painter, Adv. Appl. Math. **26**, 280 (2001).
[81] P. H. Chavanis and C. Sire, Physica A **384**, 199 (2007).